The University of Leeds LS2 9JT
Department of Earth Sciences

Departmental Office (44) - 0532 - 335222
Telex 556473 UNILDS G

Fax transmission from (44) - 0532 - 335259

Total number of pages including leader: 1

Destination (Company):
Sea Grant Office

Fax Number:
010-1-508-457-2187

For the Attention of:
Sheri DeRosa

Date:
April 9, 1992

From:
Cindy Ebinger

Account Code:
3GP

Subject:
Rungwe paper

Sender's Direct Line

44-0532-335203

Message:

Dear Ms. DeRosa,

I just returned from Uganda-apologies for the delay in replying to your fax of 19 March.

The information you requested is:

Ebinger, C., A. Deino, R. Drake, and A. Tesha, Chronology of volcanism and rift basin propagation, Rungwe province, East Africa, *Journal of Geophysical Research, 94,* 15,785-15,803, 1989.

Sea Grant Project Number NA84-AA-D-00033 R/G-11.

In addition, the following paper also cites the above grant:

Ebinger, C., Tectonic development of the western branch of the East African rift system, *Geological Society of America Bulletin, 101*, 885-903, 1989.

Please phone 0532-335222 immediately if not well received

TOTAL P.01

TRANSACTION REPORT APR- 9-92 THU 7:59 P.01

DATE	START	SENDER	RX TIME	PAGES	NOTE
APR- 9	7:58	0532 335259	55"	1	OK

Chronology of Volcanism and Rift Basin Propagation: Rungwe Volcanic Province, East Africa

C. J. EBINGER[1]

Department of Earth, Atmospheric, & Planetary Sciences, Massachusetts Institute of Technology, Cambridge

A. L. DEINO AND R. E. DRAKE

Berkeley Geochronology Center, Berkeley, California

A. L. TESHA

Ministry of Energy and Minerals, Dodoma, Tanzania

Continental rifts are segmented along their lengths into 50 to 100 km-long extensional basins, suggesting a genetic relationship with regularly segmented oceanic rifts. To investigate the spatial and temporal development of along-axis segmentation in youthful continental rifts, field, remote sensing, and K-Ar geochronology studies were conducted in four Western rift (East Africa) basins. Volcanism within the Rungwe region began in late Miocene time prior to or concurrent with the development of high-angle border faults bounding the then isolated Karonga and Rukwa basins. The Usangu and Songwe border fault segments located between the Rukwa and Karonga basins developed in mid-Pliocene and Pleistocene time, respectively. Within the northern Karonga basin, approximately 2–4 km of WSW-ENE directed "thick-skinned" extension is estimated both from extrapolation of late Pleistocene slip rates to 5 Ma and from surface fault geometries. Differential strains between these extensional basins of different ages are transmitted to adjoining segments by NW and ENE striking oblique-slip transfer faults within comparatively high-strain accommodation zones. Throws along transfer faults also accommodate 2 km (minimum) variations in depth to basement beneath adjacent basins, whereas monoclines and ramps accommodate differential uplift along the flanks of basins. The observed geometry of en echelon border fault segments linked by shorter oblique-slip transfer faults is similar to patterns predicted in numerical models of en echelon normal fault interactions [e.g., *Aydin and Pollard*, 1982]. Eruptive centers for alkali olivine basalt and phonolite flows within the Rungwe region coincide with the tips of en echelon border fault segments and with high-angle transfer faults linking discrete border fault segments. The locations of eruptive centers appear to be controlled by faults, and these centers generally have propagated northward along transfer faults during Plio-Pleistocene time. Historic eruptions near late Miocene centers located at the southern end of the transfer fault system, however, argue against a northward migration of the magma source. Thus, an along-axis propagation of "thick-skinned" lithospheric extension links once isolated basins and produces an along-axis segmentation of this youthful rift. Propagation of magmatism along transfer faults linking en echelon border faults locally contributes to the regular segmentation.

INTRODUCTION

Along the 2000 km length of the volcanically and seismically active Western rift, East Africa, approximately 100-km-long, generally asymmetric basins are bordered along one side by en echelon systems of high-angle normal faults (border fault segments) [*Crossley and Crow*, 1980; *Ebinger et al.*, 1984; *Rosendahl et al.*, 1986; *Peirce and Lipkov*, 1988; *Ebinger*, 1989a] (Figure 1). A geometrically similar along-axis segmentation is found in the Kenya and Main Ethiopian rifts, and along the length of oceanic rifts [e.g., *King*, 1978; *Macdonald and Fox*, 1983; *Reynolds*, 1984; *Bosworth*, 1985; *WoldeGabriel and Aronson*, 1987]. Distinct differences in seismic stratigraphies, amounts of subsidence, timing of volcanism, and extent of faulting between adjoining basins suggest that Western rift segments developed at different times, possibly evolving in a north-to-south direction [*Crossley and Crow*, 1980; *Ebinger et al.*, 1984]. However, constraints on the initial development and linkage of active rift basins are needed to evaluate processes contributing to the observed regular segmentation, and its permanence throughout successive episodes of rifting.

In three-dimensional rift models, strains within en echelon extensional segments are transmitted to adjacent segments by transfer faults that cross-cut the rift valley [e.g., *Burchfiel and Stewart*, 1966; *Gibbs*, 1984; *Bosworth*, 1985; *Rosendahl et al.*, 1986]. The age, orientation, displacement, and length of transfer faults within interbasinal "accommodation zones" place kinematic constraints on the direction and amount of extension within continental rifts [e.g., *Burchfiel and Stewart*, 1966; *Gibbs*, 1984]. The four isolated volcanic provinces of the Western rift coincide with accommodation zones, suggesting an intimate relationship between volcanism and faulting during the initial stages of continental rift development [e.g., *Pouclet*, 1977; *Ebinger*, 1989a, b; *Pasteels et al.*, 1989]. Geodetic and seismic observations within other volcanically active rift zones and mechanical models of dike injection indicate that magmatic processes can lead to slip along existing faults and the initiation of new faults [e.g., *Abdallah et al.*, 1979; *Rubin and Pollard*, 1988]. Thus, the spatial and temporal relationship between Western rift eruptive centers and transfer faults provides geometric and kinematic constraints on the development of continental rift basins and accommodation zones.

Basaltic and volcaniclastic sequences from the geographically remote Rungwe volcanic province (Western rift) cover accommodation zones between three asymmetric basins: the northeastward tilted Songwe basin, the northwestward tilted Usangu basin, and the northeastward tilted Karonga basin (Figure 2). Although recent multichannel seismic reflection and gravity studies have been conducted in parts of the Rungwe region, the orientation, age, and displacement of faults within the volcanic province were poorly understood [e.g., *Harkin*, 1960; *Chorowicz*,

1983; *Crossley*, 1982; *Ebinger et al.*, 1987; *Peirce and Lipkov*, 1988]. Previous estimates of the age of these rift basins range from Cretaceous to Pliocene, with the discrepancy in large part due to the paucity of geochronological data [*Dixey*, 1928; *Harkin*, 1960; *Tiercelin et al.*, 1988]. Thus, a regional stratigraphic framework was needed to study the development of transfer faults linking the Songwe, Usangu, and Karonga basins, and to evaluate a proposed along-axis propagation of rifting. Because parts of the Rungwe region were affected by one or more episode of rifting in Mesozoic time, a regional stratigraphy also was needed to distinguish between early Mesozoic faults and sedimentary sequences, and those related to Cenozoic rifting.

The specific objectives of this field, remote sensing, and K-Ar geochronology study were (1) to establish a volcanic chronostratigraphy within the Rungwe volcanic province and to correlate these dated volcanic horizons and interbedded sedimentary sequences within the Songwe, Usangu, and Karonga basins; (2) to ground check structural interpretations of Landsat 5 Thematic Mapper (TM) imagery; (3) to use the radioisotopic age data and stratigraphic correlations as constraints on the timing of fault movements within basins and accommodation zones; and, (4) to determine the time and space relationship between eruptive volcanic centers and fault systems within the Rungwe region (Figure 2). Detailed field studies were conducted in parts of these three basins during 1987 and 1989. Enhanced TM imagery were used to extend interpretations north to Lake Rukwa and south to Lake Malawi (Nyasa) where existing aeromagnetic, seismic reflection, and gravity data provide geometric constraints on subsurface faults [*Ebinger et al.*, 1987; *Specht*, 1987; *Peirce and Lipkov*, 1988]. On the basis of comparison of basin stratigraphies and age relations between eruptive volcanic centers and transfer faults, we suggest that a local along-axis propagation of faulting and volcanism between originally isolated basins contributes to the observed segmentation of the Western rift valley.

BACKGROUND

The 1300-km-wide East African plateau has been attributed to dynamic heating of the continental lithosphere above a convectively upwelling region within the asthenosphere, with regional extensional stresses largely generated by heating/thinning the subcrustal lithosphere [e.g., *Burke and Dewey*, 1973; *Turcotte and Emerman*, 1983; *Ebinger et al.*, 1989] (Figure 1, inset). The generally north-south trending Western rift valley roughly parallels the magmatically active Kenya rift located along the eastern side of the uplifted East African plateau (Figure 1). Viewed on a continental scale, the Western rift has developed within Precambrian orogenic belts surrounding Archaean cratons, suggesting that the cratonic lithosphere is stronger (Figure 3). Variations in lithospheric strength within the central African

continent indicate that rifting processes have weakened the lithosphere beneath the Rungwe region relative to the stable craton to the northwest, but the lithosphere beneath the Rungwe province maintains significant strength in extension (flexural rigidity of ~4 x 10^{23} N m, [*Ebinger et al.*, 1989]).

Faults, mylonites, and fold axes within Precambrian metamorphic basement generally strike northwest and east-west in the Rungwe region, although gneissic foliations and dikes show no preferred orientation [e.g., *Stockley*, 1948; *Spence*, 1954; *Harkin*, 1955; *Grantham et al.*, 1958; *Harkin*, 1960; *Teale et al.*, 1962; *MacFarlane*, 1963; *Ray*, 1975; *Klerkx and Nanyaro*, 1988; this study]. Northwest striking lineaments apparent in Landsat imagery from the Rungwe region (79-m resolution) previously were interpreted as part of a 1000-km-long, right-lateral transform fault system between Lakes Tanganyika and Malawi [e.g., *Chorowicz*, 1983; *Tiercelin et al.*, 1988]. The lack of teleseismic events within this 1000 km-long region, however, is atypical of other active continental transform boundaries, and new observations suggest a local WSW-ENE extension direction.

In parts of the Rungwe region, lacustrine sediments were deposited during a Triassic-Jurassic rifting episode (Karroo beds) and during a period of carbonatitic volcanism in early Cretaceous time (Dinosaur beds) [*Dixey*, 1928; *Spence*, 1954; *Harkin*, 1955; *Ray*, 1975; *Pentel'kov and Voronovskiy*, 1977; *Crossley*, 1982; *Peirce and Lipkov*, 1988] (Figure 3). Fauna preserved in basal red sandstones encountered in drill cores from the Rukwa basin and lacustrine sediments exposed along the margin of the Karonga basin suggest that Tertiary faulting and subsidence commenced in late Miocene or early Pliocene time [*Crossley and Crow*, 1980; *Kaufulu et al.*, 1981; *C. Morley*, personal communication, 1988]. Within the Rungwe volcanic province, *Harkin* [1960] identified eruptive centers for alkalic basaltic flows, and estimated a Plio-Pleistocene age for basal sequences based on the "fresh" appearance of flows. Problematically, K-Ar dates for two volcanic samples (33.11 ± 1.69 Ma and 41.64 ± 2.08 Ma) reported by *Tiercelin et al.* [1988] suggest that volcanism began 27–35 m.y. before sediments began to accumulate, and 24–30 m.y. prior to the earliest volcanism in the northern Western rift [e.g., *Bellon and Pouclet*, 1980; *Pasteels et al.*, 1989].

K-Ar Ages of Volcanic Rocks

Radiometric age determinations of 17 whole rock samples collected in 1987 were made at the Berkeley Geochronology Center using the K-Ar technique [e.g., *Dalrymple and Lanphere*, 1969; *Deino and Drake*, 1985]. Thin section examination of all samples revealed that mineral alteration was minor. For the basalts, only those samples showing fresh olivine or olivine with slight marginal alteration were dated (Table 1). Because of alteration of the glassy groundmass of sample T6C, analyses were made on an

anorthoclase separate (Table 1). Crushed samples in the 30–60 mesh size fraction were cleaned in successive 5-min. rinses of 5% HCl, 5% HF solution, and warm distilled water in an ultrasonic cleaner. Olivine phenocrysts were removed from the basalt samples prior to analyses.

All argon analyses listed in Table 1 were made using an extraction line/mass spectrometer configuration that allows replicate analyses of gas released from the fusion of a sample. For each sample (except T9C), the first gas fraction measured was used as an exploratory analysis to determine the gas volume available (see footnote, Table 1). Weight percentages of potassium were determined by wet chemical analyses using a flame photometer. The final ages are expressed in Table 1 as the weighted mean of the replicate argon analyses, and these weights are the inverse variance of the individual analyses. Standard errors were determined using a formula from *Taylor* [1982, p. 150]. The analytical precision of these measurements reflects errors in the measurement of the individual isotopes, as well as errors in the atmospheric ^{40}Ar ($^{40}Ar^*$) correction.

Development of Rift Basins

Analyses of enhanced color TM imagery (appendix) calibrated with field observations, aeromagnetic data [*Peirce and Lipkov*, 1988], seismic reflection data [*Ebinger et al.*, 1987; *B. Rosendahl*, written communication, 1987], and gravity data [*Aoki*, 1969; *Fairhead and Sowerbutts*, 1973; *Peirce and Lipkov*, 1988] were used to supplement existing 1:125,000 geological maps [*Stockley*, 1948; *Spence*, 1954; *Harkin*, 1955; *Grantham et al.*, 1958; *Harkin*, 1960; *Teale et al.*, 1962; *MacFarlane*, 1963; *Harkin and Harpum*, 1978]. Topographic maps at a scale of 1:50,000 were used as a map base throughout the study area shown in Figure 2. Where faults had not been mapped previously, offsets of upper Miocene–Recent strata, topographic relief, fault scarp morphology, occurrence of hot springs, and offsets of pre-rift basement faults and geologic contacts were used to differentiate late Cenozoic faults from older structures in the field and in TM imagery.

The Rukwa-Songwe, the Songwe-Karonga, and the Usangu-Karonga accommodation zones are shown with respect to border fault systems bounding basins in Figure 2. Chains of volcanic centers (polyphase shield complexes, pyroclastic cones, maars, tuff rings, dikes, and explosion craters) striking ENE and NNW crosscut the rift valley within accommodation zones. These chains form physiographic barriers between the Rukwa, the Malawi, and the Usangu drainage basins (Figures 2, 4, and 5). Hence, the thickness and composition of late Cenozoic sedimentary and volcanic sequences vary from basin to basin. Outcrop exposure in the relatively dry region to the north of the volcanic chain is good, whereas the southern face of the volcanic chain (Poroto Mountains) and the Livingstone escarpment are covered by rain forest. We

briefly describe below stratigraphic relations used as geometric and kinematic constraints on the development of basins, and summarize structural relations within basins and accommodation zones.

Basin Stratigraphies

Volcanic centers corresponding to the earliest volcanic sequences in the Karonga basin are difficult to identify due to erosion of the edifices and an obscuring cover of tephra and tuffs from more recent eruptions. These earliest sequences were grouped by *Harkin* [1960] as Older trachytes (Ot), phonolites (Op), and basalts (Ob), and we retain this nomenclature where eruptive centers for flows are not known. We correlate many of the dated flows with map units delineated and described by *Harkin* [1960], although we have differentiated and renamed several units based on the results of the radioisotopic age determinations (Table 1; Figures 5 and 6). Map units shown in Figure 5 represent compositionally similar suites of flows from specific volcanic centers overlying the typically altered basal sequences (Ot, Op, Ob).

Songwe basin. Based on faunal evidence and compositional similarity, we tentatively correlate red sandstones (K) overlying Karroo sequences (JR) with upper Jurassic–lower Cretaceous fluvio-lacustrine sequences (Dinosaur beds) cropping out along the western side of the Karonga basin (K; Figures 5, 6). An erosional but commonly conformable surface separates K from overlying white to tan sandstones and siltstones of Pliocene-Pleistocene age (Ns) containing pebbles and boulders of metamorphic basement. An altered basalt unit (Ob) overlying basement may have erupted during the same period as Ns, but eruptive centers for these flows probably were located within the Karonga basin [*MacFarlane*, 1963; this study]. An unconformity separates the fluvio-lacustrine sediments (Ns) from overlying volcaniclastic lake sediments (QNs*) that are interbedded with felsic tuffs (Mbeya tuffs; Mf, Mf_1) (Figure 6).

The stratigraphically lowest flow unit, a porphyritic trachyte (St), yielded an age of 0.55 ± 0.01 Ma (T6C; Figures 5 and 6). Boulders of petrographically similar trachytes within an ignimbrite (St_i) overlying QNs* near the northwestern tip of the Songwe border fault segment suggest that St_i corresponds to the same eruptive sequence (Figure 5). A 5-m-thick olivine basalt (Po) and a thin melanephelinite (Pu) are the youngest flow units within the Songwe basin (Figure 6). Olivine basalts and picrites (Sb) from isolated centers along the southern tip of the Songwe border fault segment may be chronostratigraphic with olivine basalts (Po) found at an elevation 300 m lower within the rift valley, or with petrographically similar Miocene-Pliocene basalts (Mb_p) covering the Usangu plateau (Figures 4 and 5). Tan lacustrine sandstones interbedded with ignimbrites (QNs*) overlie Ob and Po in the southern Songwe basin. The central Songwe basin is covered by unconsolidated pumiceous felsic ash and tephra that may be

correlative with felsic ash found in core data from beneath Lake Tanganyika dated at 11 ka [*Livingstone*, 1965] (T-2, Figure 2).

Southwest Usangu basin. Metamorphic basement is overlain by olivine basalts (Mb_m, Mb_p) dated at 7.10 ± 0.15 Ma (T5F) and 3.04 ± 0.04 Ma (T4D), respectively (Figure 5). Individual flows within the ~200-m-thick Ot sequence stratigraphically above Mb_m and Mb_p cannot be traced due to pervasive alteration and lack of exposure. Thickness variations and the average orientation of vesicles, however, indicate that the sequence erupted from centers located along the northeastern flank of the ENE striking Poroto Mountains (Figure 5). Trachytes (Ot) from the base of the eastern flank of Ngozi were dated at 2.2 ± 0.2 Ma, thus providing an upper age constraint on the altered trachyte sequences (Ot) in the Usangu basin (T7A, Figures 5 and 6).

Pumiceous sediments and water-deposited tuffs (QNs*) locally were deposited after Ot and before an olivine basalt unit (Po). A sample from the base of the Po sequence gave an age of 0.57 ± 0.01 Ma (T5K, Figure 5). Therefore, QNs* was deposited between 2.2 and 0.57 Ma. On the basis of compositional and stratigraphic similarity between volcaniclastic sediments (QNs*) in the Usangu basin and those in the central Songwe basin, the two sequences probably are correlative (Figure 6).

Late Pleistocene–Holocene trachyte and phonolite flows (Pp_1, Pp_2) were emitted from centers located along NNE striking normal faults within the Usangu basin (Figure 5). The youngest flows within the Usangu basin, inferred from their lack of vegetative cover, are trachyandesites (Pe) from a center along the Poroto ridge separating the Usangu and Songwe basins, and picrites (Usangu scarp basalts; Ub) emanating from a 30m-wide tephra cone located along the edge of the Usangu escarpment (T4L, Figure 5). As in the Songwe basin, much of the southwestern Usangu basin is covered with 1-10 m of altered tephra from recent eruptions.

Northwest Karonga basin. The Lower Chiwondo beds (Ns), calcareous siltstones and sandstones that contain fauna dated at 4–5 Ma overlie the Dinosaur beds (K) as well as Karroo sequences (JR), where described in Malawi [*Dixey*, 1928; *Ray*, 1975; *Kaufulu et al.*, 1981; *Crossley*, 1982] (Figures 5 and 6). Fossiliferous calcareous sandstones (Ns) containing clasts of reworked K and volcanic breccia we discovered south of Tukuyu are correlated with the Lower Chiwondo beds (Figure 5). The Upper Chiwondo beds (Ns) in Malawi contain 2.4- to 2.6-m.y.-old fauna, and are interbedded with felsic ash and phonolitic ignimbrites (Op_1) in Tanzania [*Kaufulu et al.*, 1981; *Crossley*, 1982] (Figure 5). A pink felsic tuff (Sf) containing numerous clasts of Ns lies within the Upper Chiwondo beds and extends north beneath olivine basalts (Ob_p) dated at 2.25 ± 0.07 Ma (T8D, Figure 5). A thin basaltic flow sequence (Wb) beneath Sf probably was erupted during mid-Pliocene time, based on the conformable flow contacts between Wb, Sf, and Ob_p. Picrites and alkali basalts (To), derived from the low, eroded shield complex at Tukuyu

unconformably overlying Ob_p and Sf, gave ages of 2.12 ± 0.04 Ma and 1.63 ± 0.06 Ma (T9C, T14A, Figure 5).

Much of the 2100-m-high polyphase shield complex at Rungwe was constructed in late Pleistocene time (Figure 5). Undated basalts from Rungwe (Ro) are overlain by phonolites (Rg) dated at 0.25 ± 0.01 Ma, trachytes (Rt; Harkin's Tp) dated at 49 ± 1 ka (T8A, Figure 5), and widespread trachytic ignimbrites. Stratigraphically above Ro, Rg, and Rt, numerous discrete phonolite flows (Rg_{1-7}), phonolitic tuffs, and basalt flows (Rs) from a NNW striking chain of tephra cones within the central Rungwe caldera attest to the youthfulness of the explosive Rungwe center. The generally flat-lying Pleistocene Chitimwe beds cropping out south of the accommodation zone unconformably overlie the Upper Chiwondo beds and may be chronostratigraphic with Rungwe volcanic sequences [*Livingstone*, 1965; *Crossley*, 1982; *Bishop*, 1987]. Phonolitic pumiceous tuffs (Ngana tuff; Rf) dated at 11 Ka by ^{14}C analyses are chronostratigraphic with ash layers beneath Lake Tanganyika [*Crossley*, 1982] (T-2, Figure 2). The Ngana tuff (Rf) may continue beneath Lake Malawi and correlate with one of several ash layers recovered in shallow cores [*Johnson et al.*, 1988] (86-30, 86-33; Figure 2).

Northeast Karonga basin. With an age of 7.25 ± 0.6 Ma, a phonolitic trachyte (Et; Harkin's Ot sequence) is the oldest Rungwe province volcanic sample yet dated (T13F, Figure 5). More than 200 m of altered phonolites (Ep), Et, and ignimbrites (Ep_i) cover the northern tip of the Karonga border fault segment (Figure 5). Thin undated basalt flows (Eb) from small eruptive centers located along the edge of the Elton plateau overlie Ep and basement. Eb is petrographically similar to late Miocene–Pliocene age olivine basalts (Mb_m, Mb_p) covering the Usangu plateau and step faults along the Usangu escarpment.

Basaltic volcanism within the northern Karonga basin had begun by the latest Miocene and continued to historic times; phonolites (Op) overlain by picrites (Ob_m) dated at 5.45 ± 0.21 Ma (T15B) were erupted from explosion craters south of the Kiejo shield complex. Op and Ob_m were buried by basal phonolitic-trachytic flows (Kat) from Katete dated at 2.35 ± 0.04 Ma (T11A, Figure 5). Identifiable centers for mid-Pleistocene basaltic (Kb_1; 0.42 ± 0.03 Ma) and phonolitic (Kg; 0.36 ± 0.03 Ma) activity within the Karonga basin are the shield complex at Kiejo, and maars, craters, and small eroded cones located south of Kiejo and along the Mbaka transfer fault (T10G, T10H, Figure 5). A 0.10 ± 0.11 Ma picritic flow (Kb_2) derived from one of several tephra cones located along the footwall of the Mbaka fault flowed down an existing escarpment, and flows have been faulted subsequently (T14B; Figures 5 and 7). Historic eruptions from cones located on the northern side of Kiejo (Sbt) and along the Mbaka fault attest to ongoing activity in the Usangu-Karonga accommodation zone (Figure 5).

Relationship Between Miocene-Recent Volcanism and Faulting

Songwe basin. The narrow Songwe basin is bounded on its eastern side by a 1200-m-high escarpment consisting of subparallel high-angle normal faults that rise to the level of the uplifted flank (step faults; Figure 5). Carbonatitic breccia exhumed along the Songwe scarp is presumed to have been emplaced during the same period as early Cretaceous carbonatites exposed in the Songwe basin [*Brown*, 1962; *Pentel'kov and Veronovskiy*, 1977]. Basal scarps are triangular, and the most recent movements along the Songwe escarpment are dip-slip, based on the plunge of slickenside striae [*Tiercelin et al.*, 1988; this study] (Figure 5). Eruptive volcanic centers (Sb) are located along en echelon step faults at the southern tip of the Songwe border fault segment. Vertical relief along the Songwe escarpment decreases to the north where N30°W striking faults cut Mesozoic sediments of the Rukwa trough and Neogene-Holocene lacustrine sediments [*Spence*, 1954; *Grantham et al.*, 1958] (Figure 5). The western side of the basin is a northeast dipping monocline rarely cut by late Cenozoic faults [*Grantham et al.*, 1958] (Figure 5). Thus, the regional cross-sectional morphology of the Songwe basin is that of a half-graben tilted to the northeast (Figures 3, 4, and 5).

The strikes of late Cenozoic normal faults and open fissures within the Songwe basin are approximately parallel to the Songwe escarpment (Figure 5). The North Songwe River, for example, flows northwest along the hanging wall of a southwestward dipping normal fault (Figure 5). Hot springs, tufa deposits (QNc), and eruptive centers mark northwest striking normal faults along the eastern side of the basin [*Grantham et al.*, 1958](Figure 5). The southwestern margin of the Songwe basin, where few, if any, faults displace Ob or St, is a monocline ramped down to the north (e.g., Figure 4). N20°E striking faults bounding a buried ridge link the Rukwa and Songwe extensional segments [*Peirce and Lipkov*, 1988].

Faulting and rapid subsidence in the Rukwa basin to the north of the Songwe basin began in late Miocene or early Pliocene time when Lake Rukwa covered a much broader region [*Peirce and Lipkov*, 1988; C. Morley, personal communication, 1988]. However, much of the present topography within the Songwe basin was created during a period of faulting and tilting in mid-Pleistocene time based on the following evidence. First, the commonly conformable contact between Cretaceous (K) and Neogene (Ns) sequences, and the uniform thickness of laminated, parallel beds Ns comprises, indicate that little faulting occurred prior to or during their deposition in ancient Lake Rukwa. Second, fluvio-lacustrine sequences (Ns, QNs*) thicken from 200 m to more than 5 km in the Rukwa basin, indicating that the present Songwe basin has been a topographic high relative to the Rukwa trough since late Miocene time. The lack of faunal evidence for a hydrological connection between Lake Rukwa at 790 m and Lake

Malawi at 474 m [e.g., *Grove*, 1983; *P. Williamson*, personal communication, 1987] indicates that the Songwe basin was a topographic high prior to the construction of the Ngozi shield complex (Ot) in mid- to late Pliocene time. Ns probably was deposited in erosional depressions cut into friable Mesozoic sedimentary sequences that were redeposited within the topographically lower Rukwa basin [*Grantham et al.*, 1958; *Peirce and Lipkov*, 1988; this study]. Third, sedimentary beds within Ns dip 10°-15°NE; beds within Plio-Pleistocene volcaniclastic beds (QNs*) and flow contacts (St, Po) dip less than 10° to the northeast. Fourth, northwest striking faults within the Songwe basin displace mid-Pleistocene trachytes (St), and we find few faults internal to these approximately 5-km-wide fault blocks (Figure 5). Fifth, mid-Pleistocene basalt flows (Po) followed present topographic relief, indicating some faulting had occurred prior to their eruption (Figure 5).

Southwest Usangu basin. The southwestern end of the Usangu basin near the Usangu-Karonga accommodation zone is bounded by a system of north-south striking faults dipping 60°–70°E (Figure 5). Step faults forming the 1000-m-high Usangu escarpment cut E-W and WNW striking diabase dikes and lithologic contacts within Precambrian gneissic basement [*Teale et al.*, 1962; this study]. Although shown as a 300-km-long fault on earlier maps, the topographic escarpment is less than 100-km-long, and the NE trending depression northeast of the Usangu basin probably reflects pre-rift topography (e.g., Figure 3). There is little evidence for faulting or volcanism along the flat, uplifted Usangu plateau outside the rift valley (Figure 5).

The southeastern margin of the Usangu basin is the uplifted flank of the Karonga basin, which is tilted and faulted down to the north [e.g., *Teale et al.*, 1962] (Figure 5). As in the Songwe basin, youthful-appearing volcanic centers are located along steep normal faults at the tip of the Usangu escarpment. For example, an uneroded scoriaceous cone (Ub) is located along a fault bounding the escarpment, and picritic flows from this cone flowed away from the rift valley along the back-tilted rift flank (T4L, Figure 5). Numerous trachytic and phonolitic tuff rings and pyroclastic cones (Pp_{1-2}) coincide with the footwalls and hanging walls of NNE striking normal faults near the Usangu-Karonga accommodation zone (Figures 2 and 5).

On the basis of aeromagnetic data interpretations, *Peirce and Lipkov* [1988] suggest that metamorphic basement may be buried by 2 km of sedimentary and volcanic sequences within the Usangu basin. However, our observations do not support this intepretation: Mesozoic sediments exposed elsewhere in the Rungwe province are not observed at the surface in the southwest Usangu basin, and the Usangu basin is characterized by a Bouguer gravity high relative to the volcanic province to the west (Figure 8).

The following observations indicate that the Usangu escarpment developed after 3 Ma (after Mb_p), that the Usangu basin was a

topographic depression by mid-Pliocene time, and that normal faulting/tilting predominantly occurred in Pleistocene time. First, a sequence of Mb_m, scoria, talus, and olivine basalts (Mb_p) is repeated along step faults forming the Usangu escarpment, indicating that initial faulting along the Usangu border fault segment postdates mid-Pliocene time. Boulders of metamorphic basement and basalt fill steep gorges along this active fault scarp, but there is little evidence that basalts flowed down a preexisting escarpment. Plio-Pleistocene volcaniclastic sequences (QNs*) unconformably overlie Mb_p at the base of the Usangu escarpment and dip 20°–30° toward the Usangu border fault segment. This indicates that faulting and basinal subsidence began after 3 Ma. Second, trachytic flows (Ot) from the Poroto chain cover the southwestern Usangu basin but are absent along escarpments bounding the basin, implying that the rift valley walls were elevated above the basin in mid-Miocene time. Third, basal trachytes (Ot) and late Pleistocene flows (Po, Pe, Pp_1) within the Usangu basin are offset by normal faults striking N20°E and N40°W, and stream drainage within the basin largely is controlled by these normal faults (Figure 5). Finally, the thickness of volcaniclastic sequences (QNs*) above Po (mid-Pleistocene) is greatest along the downthrown side of 1 to 5-km-wide tilted fault blocks, indicating that syndepositional fault block rotations occurred during late Pleistocene time.

Karonga basin. The 100-km-long Karonga basin is bounded along its eastern margin by 1 to 2-km-wide step faults dipping 60°–75°SW, known as the Livingstone escarpment (Figure 5). Throws along N20°-30°W striking normal faults increase to the south where Lake Malawi occupies the spoon-shaped Karonga basin [*Specht*, 1987; *Ebinger et al.*, 1987]. Faults bounding the Karonga basin splay out at the northern tip of the escarpment, contributing to the curvilinear geometry of the Karonga border fault segment (Figures 4, 5). Spurs are faceted, and the innermost fault zone is characterized by youthful-appearing triangular scarps. Slickenside striations along the base of the escarpment indicate that the most recent movements along the Karonga border fault segment have been oblique-slip [*Tiercelin et al.*, 1988; this study]. The opposite side of the northern Karonga basin is bordered by en echelon normal faults with small throws, relay ramps [e.g., *King*, 1978], and ENE dipping monoclines [*Crossley and Crow*, 1980] (Figure 5).

Within the northern Karonga basin, high-angle normal faults cutting late Cenozoic sedimentary and volcanic sequences generally strike N-S to NNW (Figure 5). Resistant ridges of southeastward dipping To and Op_1 mark footwalls of tilted fault blocks north of Lake Malawi (Nyasa) where much of the relief is erosional (Figure 5). Faults offsetting acoustic basement beneath the central Karonga basin strike northwest and north-south [*Ebinger et al.*, 1987; *Specht*, 1987]. Unfortunately, no deep drill data are available to

correlate the 2 to 5(?)-km-thick sedimentary sequences beneath the eastern Karonga basin with volcanic sequences we have dated.

The following observations indicate that faulting along the northern end of the Karonga border fault segment began between 7.25 Ma and 5 Ma, and that a lake basin had formed by mid-Pliocene time. First, once contiguous late Miocene phonolitic trachytes (Et) are cut by high-angle border faults with a cumulative downthrow of more than 1500 m. A lake filled the northern Karonga basin by 5 Ma when lacustrine sediments (Ns) were deposited along the northwestern side of the Karonga basin and basalts were erupted along an intrabasinal fault (Ob_m) [*Kaufulu et al.*, 1981]. The large length to height ratios of numerous explosion craters (Ob_m, Ob_p, Kb) located along the hanging wall of the Mbaka transfer fault are characteristic of craters that formed in shallow water or in wet sediments [e.g., *Heiken*, 1971; *Wood*, 1980]. Their morphology indicates that Lake Malawi extended further north in mid-Pliocene time when the Chiwondo beds were deposited. The primarily postdepositional faulting and wedge-shaped geometry of volcaniclastic sequences (Ns*) suggests that faulting and SSE directed tilting within the northern Karonga basin began in mid-Pliocene time [*Bishop*, 1987; this study].

Songwe-Karonga Accommodation Zone. The 40-km-wide, 50-km-long Songwe-Karonga accommodation zone is a structural high relative to the Songwe and Karonga basins, although volcanic construction augments topographic relief in this zone (e.g., Figure 4). On the basis of an extrapolation of dips of bedding contacts in the Tertiary sequences, less than 500 m of volcanics have accumulated along the hanging walls of 5 to 10-km-wide eastward tilted fault blocks, excluding the shield complexes at Ngozi, Rungwe, and Kiejo (e.g., Figure 9). Metamorphic basement exposed along the N50°W striking Mbaka transfer fault system and the closed-contour Bouguer gravity low west of the Mbaka fault zone suggest that Mesozoic sediments are thin to absent east of the Mbaka transfer fault (Figures 5, 8, and 9).

Throws along the Mbaka fault partially accommodate the 2600 m (minimum) elevation difference between basement beneath the Songwe basin (~1100 m) and the northern Karonga basin (~1500 m or more). The plunge of slickenside striations (70° to N70°E) along the Mbaka fault, which is oriented 20°–30° from the NNW strike of the Karonga border fault segment, indicates that the most recent displacements along the Mbaka fault have been oblique-slip. From observations within the accommodation zone, throws along at least three ENE striking transfer faults also contribute to the elevation difference between the Songwe and Karonga basins (A, B, C, Figure 10). Several N70°–80°E striking normal faults offset Miocene-Pleistocene basalts (Mb_m, Mb_p, Ot, Po) and QNs* between a northern projection of the Karonga border fault segment and the tip of the Songwe border fault segment (A, Figure 10). Within one highly brecciated fault zone, conformable contacts within QNs* dip 20°–30°NW toward the escarpment, suggesting

that high-angle ENE striking faults developed in Quaternary time. The narrow zone of ENE striking faults has been offset by more recent movements along northwest striking Songwe border faults, producing a grid fault pattern east of Mbeya (Figures 4 and 5).

Considering the coincidence of volcanic centers and faults throughout the Rungwe province, the ENE trending topographic ridge of eroded volcanic centers (Poroto Mountains) probably marks a buried fault along strike with the southern margin of the Usangu basin (B, Figure 10). Late Cenozoic sediments (Ns-QNs*) thicken from less than 500 m along K–K' to over 2 km beneath the central Karonga basin, indicating that a southward dipping normal fault system crosscuts the northern Karonga basin. Closely-spaced high-angle ENE striking normal faults south of the volcanic province are characterized by drag folds, and Pliocene–Recent sequences dip 20° to the southeast along this hinge zone (C, Figures 5 and 10). A narrow gravity high associated with an ENE striking fault system along the western margin of the Karonga basin coincides with the eastward offsets in rivers (Figures 5 and 8). Thus, we interpret a buried ENE striking oblique-slip fault downthrown to the south ~10 km north of Lake Malawi (C, Figure 10). A lake covered the topographic ridge separating the two basins in Pleistocene time (QNs*), placing a maximum age constraint on the Songwe-Karonga accommodation zone.

Nearly all of the eruptive centers within the Rungwe volcanic province lie within the Songwe-Karonga accommodation zone where Miocene–Holocene centers generally coincide with the tips of border faults and transfer faults (Figures 2 and 10). For example, small pyroclastic cones and fissures (Sb) have formed along en echelon step faults at the tip of the Songwe escarpment, and Miocene–Pliocene centers (Et, Eb, Ot) are located along the tip of the Karonga border fault segment (Figures 5 and 10). Alignments of lower Pliocene craters (Ob_P) parallel to the N50°W striking Mbaka transfer fault suggest that it served as a conduit for basalts during mid-Pliocene time (Figures 5, 10). Explosive products within Op and Op_i indicate that eruptive centers were located near the southern margin of the volcanic province. Eruptive centers at Katete, Kiejo, and Tukuyu were constructed along northwest striking faults paralleling the Mbaka transfer fault during mid- to late Pliocene time. A N35°W striking chain of maars and uneroded tephra cones overlying mid-Pliocene trachytes (Ot) extends north from the Pleistocene Rungwe center to the southern tip of the Songwe border fault segment. Thus, eruptive volcanic centers propagated north from the northern Karonga basin toward the tip of the Songwe border fault segment during Pliocene-Holocene time, although volcanic activity continued through historic times at Pliocene centers located along the southern Mbaka transfer fault system (e.g., historic flow Sbt from Kiejo).

Usangu-Karonga accommodation zone. As in the accommodation zone between the Karonga and Songwe basins, the Usangu-Karonga accommodation zone is a structural high relative to the

shallow Usangu basin and the deep Karonga basin (Figure 5, inset). Here, subvertical north-south striking faults with small throws (< 6 m) and east dipping faults striking N10°–20°W link the eastward dipping Usangu border fault segment and the southwestward dipping Karonga border fault segment (Figure 5). Differential movements between the Usangu and Karonga rift segments also may be compensated by N35°W striking oblique-slip faults within the Songwe-Karonga accommodation zone. Along the southwestern Usangu basin, a northward dipping faulted monocline drops the uplifted flank of the Karonga basin down into the Usangu basin.

Identifiable eruptive centers for Quaternary flows (Po, Pp_{1-2}) within the Usangu basin are most numerous within and near the Usangu-Karonga accommodation zone (Figures 5 and 10). Based on the correlation between the location of volcanic centers and a Bouguer gravity low, we suggest that the gravity anomaly coinciding with the Usangu-Karonga accommodation zone is due to the presence of low-density magmatic material at crustal levels (Figure 8).

Miocene-Recent Development of Basins and Accommodation Zones

The 17 age determinations, supported by structural and stratigraphic relations, indicate that the onset of volcanism within the Rungwe province in late Miocene time occurred much later than previously reported by *Tiercelin et al.* [1988]. Although ages in altered basal sequences are admittedly sparse, late Miocene-Pleistocene ages that we determine are stratigraphically compatible with existing age constraints from the Rungwe region (e.g., Figure 6). For example, the Songwe tuff (Sf) lies within the Upper Chiwondo beds which contain fauna dated at 2.6–2.4 Ma [*Kaufulu et al.*, 1981], and Sf is overlain by a flow dated at 2.25 ± 0.07 Ma (Ob_p). The maximum ages that we determine fall within the range of maximum ages of volcanic sequences found in the northern Western rift (<12 Ma) and in the southern Kenya rift (<5 Ma) [*Crossley and Knight*, 1981; *Pasteels et al.*, 1989]. Thus, the radioisotopic age determinations are consistent with paleontological age constraints and volcanic histories in other parts of the East African rift system.

Structural control of volcanism is evident within the Songwe, Usangu, and Karonga basins throughout their development in late Miocene–Recent time (e.g., Figure 10). With rare exceptions, eruptive volcanic centers are located along the tips of border fault segments, along transfer faults within accommodation zones, and in alignments crosscutting the rift valley probably marking buried faults (Figures 5, 7, and 10). Because faulting and magmatic processes are interactive and repetitive, we assume that the coincidence of eruptive centers and faults persisted throughout the development of the Rungwe volcanic province. We can therefore

use the age of volcanic sequences to constrain the development of border and transfer faults.

The following comparison of kinematic constraints from the Songwe, Usangu, and Karonga basins and the accommodation zones between basins illustrates their diachronous, but similar, development, and a local propagation of faulting, volcanism, and basin subsidence between the originally isolated Karonga and Rukwa border fault segments. These relations are illustrated schematically in Figures 10 and 11 and summarized below.

Initiation of Border Fault Segments

The occurrence of volcanic units along the uplifted flanks of the Usangu and Karonga basins and petrologically similar basalts downfaulted along the escarpments places constraints on the maximum age of border fault segments. Initial faulting along the Karonga border fault segment occurred after 7.25 Ma (Et); faulting along the Usangu border fault segment occurred after 7 Ma (Mb_m) and probably after 3 Ma (Mb_p), if the upper basalts cut by step faults along the Usangu escarpment are correlative with Mb_p (Figure 11). No geochronological constraints are available to date the initiation of faulting along the Songwe border fault segment, but observations discussed below suggest that faulting began in Pleistocene time.

Initial Basinal Subsidence and Faulting

Upper Miocene basalts from centers within the Karonga basin (Ob_m) and Lower Pliocene lacustrine sequences (Ns) exposed along the western side of the Karonga basin indicate that faulting and subsidence in the Karonga basin began at ~5 Ma. Sediments also began to accumulate within the Rukwa basin to the north of the Songwe basin between 5 and 6 Ma [C. Morley, personal communication, 1988] (Figure 11a). Within the Usangu basin, a topographic depression existed prior to the eruption of trachytes (Ot) in mid-Pliocene time. However, the attitudes of and thickness variations within Plio-Pleistocene sequences (QNs*) indicate that faulting and tilting within the Songwe basin did not begin until mid-Pleistocene time (Figure 11c).

Development of Basinal Asymmetry

Excluding flows from shield complexes, late Pliocene–Recent volcanic sequences within the Karonga basin (To, Kb, Kg, Kat) regionally were directed to the east and south, indicating that tilting in the spoon-shaped Karonga basin had begun by late Pliocene time. Asymmetry within the Usangu basin probably developed in early Pleistocene time when general flow directions changed from northeast (Ot) to northwest (Po, Pe), or toward the Usangu border fault segment. Within the gently northeastward tilted Songwe basin, Pleistocene olivine basalts (Po) generally flowed to the southwest toward the older Rukwa basin, following erosional relief

in the Dinosaur beds (Figure 5). These relations suggest that asymmetry within the Songwe basin developed in late Quaternary time.

Development of Accommodation Zones

We infer that transfer faults, monoclines, and ramps now linking the Songwe and Karonga basins were operative in mid-Pliocene time, and that volcanism and faulting along transfer faults continue through historic times (Figure 11). The Poroto volcanic chain developed during mid-Pliocene time, or approximately the same time as extensional faulting began within the Usangu basin (Figure 11b). Northwest striking transfer faults marked by chains of Quaternary eruptive centers crosscut the mid-Pliocene Poroto chain and are apparently younger. Hence, the inferred ENE striking transfer fault beneath the Poroto Mountains may have linked the eastward dipping Usangu border fault with the southwestward dipping Karonga border fault, prior to Pleistocene extension within the Songwe basin. ENE striking transfer faults at the southern tip of the Songwe border fault segment developed in Pleistocene time (a, Figure 10), or much later than ENE striking transfer faults in the northern Karonga basin (Figure 11). Thus, NW striking and ENE striking transfer faults linking the Songwe and Karonga border fault segments apparently propagated to the north. The Pliocene-age Mbaka transfer fault probably marked the northern termination of the Karonga basin prior to extension in the Songwe basin (Figure 11b).

Localization of Volcanic Centers

During Plio-Pleistocene time, eruptive volcanic centers became located more central to basins, and centers propagated northward along border and transfer fault systems linking the originally isolated Rukwa and Karonga basins. First, late Miocene volcanic centers (Et, Eb, Mb_m) were located near the outermost fault bounding the Usangu and Karonga basins, whereas most Pliocene-Holocene centers are located along steeply dipping normal faults within the rift valley (Figure 10). A comparison of ages of eruptive centers shows a northward propagation of volcanic activity within the Songwe-Karonga accommodation zone: late Miocene to mid-Pliocene centers (Ob_m, Ob_p, Kb) are found only at the southern end of the Mbaka transfer fault, whereas Pleistocene-Holocene centers (Po, Rg_{1-7}, Pe) are more numerous along the northern continuation of the northwest striking Mbaka fault (e.g., Figures 5 and 10). Eruptive centers along transfer faults linking the Usangu and Karonga border fault segments show a similar northward propagation in Plio-Pleistocene time, with youthful cones located along the northern end of the Mbaka transfer fault zone. There is no indication in seismic reflection profiles and aeromagnetic data that buried volcanic centers lie beneath the central Karonga basin [e.g., *Ebinger et al.*, 1987]. Thus, although faults bounding the

Karonga basin have been active since late Miocene time, magmatic products preferentially propagated northward along northwest and ENE striking border and transfer faults in Pleistocene time. Historic flows from centers less than 10 km from a late Miocene explosion crater located at the southern margin of the volcanic province (Ob_m, Kb_2), however, argue against a northward migration of the magma source during Plio-Pleistocene time.

Timing of Rift Flank Uplift

Uplift of the 100 to 200-km-wide regions flanking the Songwe, Usangu, and Karonga basins has tilted Miocene and Pliocene volcanic units (Et, Eb, Mb_m) away from the present axis of the rift valley. Thus, initial flow sequences erupted onto a surface of low relief, and rift flank uplift postdates initial volcanism. The morphology of the innermost step fault bounding the eastern Karonga basin is the most youthful of the step faults, and the oldest volcanic center (Et) was located along the outermost, but now inactive border fault (Figure 9). These relations indicate that the basin has narrowed with time.

TECTONIC MODEL OF THE RUKWA-MALAWI REGION

Few data currently are available to constrain the direction(s) of extension within the Western rift, in part due to difficulties in distinguishing between Precambrian-Mesozoic and late Cenozoic strains within metamorphic basement [e.g., *Chorowicz*, 1983; *Morley*, 1989; *Ebinger*, 1989*a*]. Within the Rungwe province, border and transfer faults generally crosscut earlier mylonites, dikes, and tectonic contacts, commonly at small angles where reactivation of earlier weaknesses would be expected [e.g., *Handin*, 1969]. Thus, rift faults do not appear to be controlled by these preexisting weaknesses. WSW-ENE, E-W, and WNW-ESE focal mechanism solutions determined for eight earthquake epicenters located within the Western rift only loosely constrain present-day extension directions [*Fairhead and Girdler*, 1969; *Fairhead and Stuart*, 1982; *Shudofsky*, 1985]. Because propagation and abandonment of border and transfer faults implies rotation of crustal blocks within accommodation zones, extension directions may be applicable only locally and during a particular time interval [e.g., *Strecker and Blisniuk*, 1989]. Therefore, we have attempted to use only Pleistocene indicators to evaluate a local extension direction. Within the Rungwe province, both the strike of transfer faults linking northwest striking border fault segments and slip directions along the Mbaka fault support a WSW-ENE extension direction during Quaternary time (Figure 12). Near-vertical slickenside striae along Songwe basin border faults indicate that the most recent movements along these NNW striking faults have been dip-slip, also supporting a WSW-ENE extension direction [*Tiercelin et al.*, 1988; this study].

In the uplifted regions adjacent to the rift, differential erosion enhances lithologic and inactive structural contacts in metamorphic basement apparent as lineaments in Landsat imagery, particularly in directions parallel and orthogonal to the strike of border faults. We find no evidence, however, for late Cenozoic faulting along the uplifted flanks of basins, except where en echelon border fault segments overlap and interact (e.g., Rukwa and Songwe border fault segments). These observations indicate that little or no crustal extension has occurred beneath the uplifted rift flanks outside the inner-facing border faults bounding the rift valley.

Assuming plane strain, late Cenozoic crustal extension measured across the southern Songwe-Karonga accommodation zone is 2.7–3.5 km (5-9%) (K–K', Figure 9). Late Pleistocene ankaramites (Kb_2) have been displaced 50-70 m to the southwest along the Mbaka transfer fault in the past 0.10 Ma, corresponding to ENE-directed extension rates of 0.5–0.7 mm/yr (Figures 5, 7, and 9). Assuming that the Karonga basin developed at approximately 5 Ma, an extrapolation of late Pleistocene slip rates to this time interval predicts 2.5–3.5 km of extension, or approximately the same amount estimated from surface fault geometries along K–K' (Figure 9). These values fall within the range of extension estimates of 3–11% within the northern and central Western rift [*Morley*, 1988; *Ebinger*, 1989*a, b*].

Considering the significant strength of the lithosphere beneath the Rungwe region noted earlier, the apparent abandonment of border faults and progressive narrowing of the Karonga basin can be explained by flexural uplift of the footwall as an isostatic response to the topographic "hole" of the extensional basin [e.g., *Buck*, 1988; *Weissel and Karner*, 1989]. The depth to detachment within the northern Karonga basin estimated from a balanced cross section [e.g., *Gibbs*, 1983] of K–K' is 20 km or more, indicating that the tips of steep border faults within the accommodation zone remain steep to lower crustal levels. With continued uplift and rotation of the footwall away from the rift valley, a new fault may be generated directly above the steep detachment and inboard of the older fault [*Buck*, 1988] (e.g., Figure 9, inset).

Integrating these findings with existing observations from the Tanganyika-Rukwa-Malawi region, 50- to 100-km-long en echelon border fault segments striking north-south and northwest are linked by WSW-ENE striking transfer faults that crosscut the rift valley, and by NW striking oblique-slip faults (Figure 12). We find little evidence for a late Cenozoic NW-SE extension direction and northwest striking transform fault zone proposed by *Chorowicz* [1983] and *Tiercelin et al.* [1988]. Instead, the geometry of these high-angle fault systems produces a regular along-axis segmentation of the rift valley.

Consistent patterns in the chronology of volcanism, faulting, subsidence, and rift flank uplift are apparent in a comparison of age constraints from the Songwe, Usangu, and Karonga basins (Figure 13). In stage 1, alkali olivine basalts and/or phonolites erupt onto a

surface of low relief. Displacements along border faults offset the originally flat-lying flows, producing a terrace of basalt flows capping en echelon step faults, and basin downwarping commences. In stage 2, faulting and flexural warping produces <100 km-wide topographic depressions that begin to fill with sedimentary and volcanic sequences. The active border fault is located inside the older fault, and a new terrace is formed. By Stage 3, eruptive volcanic centers localize to transfer fault systems within inner-facing border faults. Spoon-shaped basins subside, and the zone of maximum subsidence progressively narrows with collapse of the hanging wall and flexural uplift of the footwall. This pattern began first in the Rukwa and Karonga basins (6–7 Ma), followed by the Usangu basin (2–3 Ma), and lastly the Songwe basin (1–2 Ma), with transfer faults propagating eventually to link en echelon border fault segments (Figure 11). The shallow Usangu basin could mark a "failed" rift arm that was abandoned when the Rukwa and Karonga extensional basins were linked via the Songwe border fault segment in Plio-Pleistocene time.

Considering that the combined subsidence and flank uplift vary from less than 1 km to more than 5 km between basins, ENE and NW striking transfer faults, relay ramps, and monoclines actively accommodate differential horizontal and vertical displacements between adjacent extensional segments bounded by steep, deeply-penetrating normal faults. For example, normal faults on the southeastern side of the Usangu basin accommodate uplift along the flanks of the Karonga basin, as well as subsidence and extension within the Usangu basin.

DISCUSSION

Kinematic constraints on the development of the Rukwa, Songwe, Usangu, and Karonga basins and accommodation zones between these basins indicate that extensional segments develop at different times and transfer faults propagate to connect originally isolated basins (e.g, Figure 11). In plan view, the geometry of propagating high-angle border faults, transfer faults, and eruptive volcanic centers from late Miocene time to the present day are similar to patterns predicted by theoretical models of en echelon fault interactions [e.g., *Aydin and Pollard*, 1982; *Pollard and Aydin*, 1984].

Numerical models of en echelon normal faults (border faults) predict an increase in stress in the region between faults due to the mechanical interaction of their tips, and faults linking the two cracks are initiated [e.g., *Aydin and Pollard*, 1982; *Pollard and Aydin*, 1984]. These models predict linkage by normal faults (transfer faults) that are much shorter in length than the border fault segments [e.g., *Aydin and Pollard*, 1982]. On the basis of state-of-stress calculations within the homogeneous media surrounding the en echelon normal faults, transfer faults strike oblique to border

fault segments in a geometry similar to that observed in the Rungwe volcanic province. This is in contrast to the more stable and efficient geometry of propagating vertical cracks (oceanic ridges) that are linked by strike-slip faults striking nearly orthogonal to the cracks (transform faults). For example, the 50 to 100-km-long en echelon Karonga and Songwe border fault segments are linked by 20 to 30-km-long oblique-slip normal faults, producing a dogleg rift geometry.

Within the Rungwe volcanic province, eruptive centers at the tips of border fault segments and along high-angle ENE and NW striking transfer faults cross-cutting the rift valley correlate with regions where models predict deviatoric tensile stress concentrations [*Aydin and Pollard*, 1982; *Pollard and Aydin*, 1984]. By analogy to these fracture mechanics models, magma appears to propagate along with transfer faults linking border fault segments within the Rungwe region. We anticipate, however, that prerift lateral heterogeneities in the crust beneath the Rungwe volcanic province may also influence fault geometries near the tips of propagating normal faults. Based on depth to detachment estimates of ~20 km and the coincidence of volcanic centers with the tips of border fault segments and transfer faults, these faults provide ready conduits for the ascent of magma to the surface (Figure 9). The absence of volcanic centers along the central parts of border faults and basins may indicate that the tips of border faults remain steep to deeper crustal levels than do central border fault segments, or may reflect the closer spacing of faults within accommodation zones. Because Holocene centers are located near late Miocene centers within the central rift valley, an along-axis migration of the magma source probably has not driven the border fault propagation. Amagmatic parts of the Western rift exhibit a geometrically similar along-axis segmentation, suggesting that magmatic processes facilitate, but are not prerequisites for, propagation and linkage of en echelon border fault segments.

CONCLUSIONS

Structural observations, stratigraphic relations, and geochronological data, integrated with existing geological and geophysical data, indicate that volcanism began in late Miocene time within the Rungwe province. This volcanism occurred immediately preceding or coincident with the development of northwest striking high-angle border faults bounding the originally isolated Karonga and Rukwa basins. The Karonga and Rukwa border fault segments formed between 7.25 and 5 m.y. ago, the Usangu border fault segment developed between 3 and 2 m.y. ago, and subsidence along the Songwe border fault segment had occurred by 0.5 Ma. Although individual basins developed diachronously, each followed a similar sequence of (1) initial border fault development; (2) asymmetric basin subsidence/flank uplift, and development of monoclines opposite the border faults;

and, (3) continued subsidence and tilting along intrabasinal faults with flexural upwarping of the rift flanks, enhancing basinal asymmetries.

Differential vertical and horizontal movements between basins of different ages lying at different elevations are transmitted to adjacent rift segments by transfer faults, ramps, and monoclines within accommodation zones. Numerical models of en echelon normal faults also predict similar border and transfer fault geometries and stress concentrations within accommodation zones [*Aydin and Pollard*, 1982; *Pollard and Aydin*, 1984]. Thus, the geometrical arrangement of border and transfer faults along the length of the Western rift produces approximately 100 km-long spoon-shaped basins.

An along-axis propagation of volcanism also contributes to the regular segmentation of the Western rift valley. Eruptive volcanic centers propagated northward along transfer faults linking the older Karonga basin with the Songwe basin during Plio-Pleistocene time. The coincidence of volcanic centers and comparatively high-strain accommodation zones suggests that steep, deeply penetrating border and transfer faults facilitate the ascent of magma to the surface. However, the geometry of transfer faults linking en echelon basins in the Rungwe province may rotate with time due to interactions between adjacent propagating border fault segments and with extension in newly formed basins. Transfer fault systems striking obliquely to border fault segments in youthful rifts may evolve to a more orthogonal geometry during later episodes of extension, or with the onset of true seafloor spreading.

Appendix 1

The Landsat 5 Thematic Mapper (TM) image used in this study covers a 170-km by 185-km region. Standard radiometric and geometric corrections were made at the EROS processing center, and images are displayed using a space oblique Mercator projection that preserves length and angular relations. Digital data were processed to enhance faults and lineaments and to distinguish volcanic units using a variety of filtering, color ratioing, and contrast stretching techniques. TM image is Y-50850-07204 (path 169, row 66). Quality of data is excellent; cloud cover was less than 10%. Reproduced by permission of EOSAT.

Acknowledgments. The field study was conducted in collaboration with the University of Dar es Salaam, the Ministry of Energy and Minerals (Tanzania), and the Tanzanian National Scientific Research Council. Without the assistance of J. Nanyaro, L. Lyaru, S. Townsend, J. and R. Knight, L. Willey, U. Aswathanarayana, P. Eeckelers the field research would have been impossible. We thank T. Becker and P. Youngman for their aid in the K-Ar analyses. Comments by D. Harding, B. Marsh, L. Higgins, C. Morley and the reviewers improved the manuscript. We thank Mobil, Amoco, Project PROBE, Petro-Canada, and D. Fairhead for use of unpublished information. This project was supported by Mobil Exploration Production Services, Geological Society of America Student Research grant 3754-87, NASA RTOP 677-43-27, Sea Grant NA84-AA-D-00033R/G-11), and NSF grant EAR-84-18120.

REFERENCES

Abdallah, A., V. Courtillot, M. Kasser, A.-L. LeDain, J.-C. Lépine, B. Robineau, J.-C. Ruegg, and P. Tapponnier, Relevance of Afar seismicity and volcanism to the mechanics of accreting plate boundaries, *Nature, 282*, 17–23, 1979.

Aoki, H., Gravity measurements of rift valleys in Tanzania, *J. Earth Sci., Nagoya Univ., 17*, 169–188, 1969.

Aydin, A., and D. Pollard, Origins of the zig-zag pattern of normal faults, *Geol. Soc. Am. Abstr. Programs, 14*, p. 436, 1982.

Bellon, H., and A. Pouclet, Datations K-Ar de quelques laves du Rift-ouest de l'Afrique Centrale: Implications sur l'évolution magmatique et structurale, *Geol. Rundsch., 69*, 49–62, 1980.

Bishop, M. G., Clastic depositional processes in response to rift tectonics in the Malaŵi rift, Malaŵi, Africa, 112 pp., M.S. thesis, Duke Univ., Durham, N. C., 1987.

Bosworth, W., Geometry of propagating continental rifts, *Nature, 316*, 625–627, 1985.

Brown, P. E., The tectonic and metamorphic history of the Precambrian rocks of the Mbeya region, Southwest Tanganyika, *Q. J. Geol. Soc. London, 471*, 295–314, 1962.

Buck, W.R., Flexural rotation of normal faults, *Tectonics, 7*, 959–973, 1988.

Burchfiel, B. C., and J. Stewart, The "pull-apart" origin of Death Valley, California, *Geol. Soc. Am. Bull., 77*, 439–442, 1966.

Burke, K., and J. F. Dewey, Plume-generated triple-junctions: Key indicators in applying plate tectonics to old rocks, *J. Geol., 81*, 406–433, 1973.

Cahen, L., and I. Snelling, *The Geochronology and Evolution of Africa*, 591 pp., Clarendon, Oxford, 1984.

Chorowicz, J., Le rift est-africain: Début de l'ouverture d'un océan?, *Bull. Cent. Réch. Explor. Prod. Elf-Aquitaine, 7*, 155–162, 1983.

Cowan, L M., and H. N. Pollack, Gravity in Zambia, *Nature, 266*, 615–617, 1977.

Crossley, R., Late Cenozoic stratigraphy of the Karonga area in the Malaŵi rift, in *Paleoecology of Africa and the Surrounding Islands, S. Afr. Soc. Quat. Res., 15*, edited by J.A. Coetzee and E.M. van Zinderen-Bakker, pp. 139–144, A. A. Balkema, Rotterdam, 1982.

Crossley, R. and M. J. Crow, The Malaŵi rift, in *Geodynamic Evolution of the Afro-Arabian Rift System*, pp. 77–87, Accad. Naz. Lincei, Rome, 1980.

Crossley, R., and R. M. Knight, Volcanism in the western part of the rift valley in southern Kenya, *Bull. Volcanol., 44-2*, 117–128, 1981.

Dalrymple, G. B., and M. A. Lanphere, *Potassium-Argon Dating*, 258 pp., W. H. Freeman, San Francisco, Calif., 1969.

Daly, M. C., J. Chorowicz, and J. D. Fairhead, Rift basin evolution in Africa: The influence of reactivated steep basement shear zones, in *Inversion Tectonics, Spec. Publ.*, edited by M.A. Cooper and G. Williams, Geological Society of London, in press, 1989.

Deino, A. L., and R. E. Drake, Improved calibration methods and error estimates for ^{40}K-^{40}Ar dating of young rocks, Ph.D. disseration, part III, pp. 433–454, Univ. of Calif., Berkeley, 1985.

Dixey, F., The Dinosaur beds of Lake Nyasa, *Trans. R. Soc. S. Afri., 16*, 54–67, 1928.

Ebinger, C. J., Tectonic development of the western branch of the East African rift system, *Geol. Soc. of Am. Bull., 101*, 952–967, 1989a.

Ebinger, C. J., Geometric and kinematic development of border faults and accommodation zones, Kivu-Rusizi rift (Africa), *Tectonics, 8*, 117–133, 1989b.

Ebinger, C. J., M. J. Crow, B. R. Rosendahl, D. A. Livingstone, and J. LeFournier, Structural evolution of Lake Malawi, Africa, *Nature, 308*, 627–629, 1984.

Ebinger, C., B. Rosendahl, and D. Reynolds, Tectonic model of the Malawi rift, Africa, in *Sedimentary Basins Within the Dead Sea and Other Rift Zones*, edited by Z. Ben-Avraham, *Tectonophysics, 141*, 215–235, 1987.

Ebinger, C. J., T. D. Bechtel, D. W. Forsyth, and C. O. Bowin, Effective elastic plate thickness beneath the East African and Afar plateaux and dynamic compensation for the uplifts, *J. Geophys. Res., 94*, 2883–2901, 1989.

Fairhead, J. D. and R. W. Girdler, How far does the rift system extend through Africa?, *Nature, 221*, 1018–1020, 1969.

Fairhead, J. D., and W. Sowerbutts, Catalogue of Tanzania gravity data to December, 1969, Univ. of Newcastle-upon-Tyne, England, 1973.

Fairhead, J. D., and G. Stuart, The seismicity of the East African rift system and comparison with other continental rifts, in *Continental and Oceanic Rifts, Geodyn. Ser., vol. 8*, edited by G. P. Palmason, pp. 41–61, AGU, Washington, D. C., 1982.

Gibbs, A. D., Balanced cross-section construction from seismic sections in areas of extensional tectonics, *J. Struct. Geol., 5*, 153–160, 1983.

Gibbs, A. D., Structural evolution of extensional basin margins, *J. Geol. Soc. London, 141*, 609–620, 1984.

Grantham, D. R., E. O. Teale, A. M. Spurr, D. A. Harkin, and P. E. Brown, Quarter degree sheet 224 (Mbeya), Geol. Surv. of Tanganyika, Dodoma, 1958.

Grove, A. T., Evolution of the physical geography of the East African rift valley region, in *Evolution, Time, and Space: The Emergence of the Biosphere* edited by R. W. Sims, J. H. Price, and P. E. S. Whalley, pp. 115–155, Academic, San Diego, Calif., 1983.

Handin, J., On the Coulomb-Mohr fracture criterion, *J. Geophys. Res., 74*, 5343–5348, 1969.

Harkin, D. A., The geology of the Songwe-Kiwira coalfield, Rungwe District, *Tanganyika Geol. Surv. Dep. Bull. 27*, 33 pp., 1955.

Harkin, D. A., The Rungwe volcanics at the northern end of Lake Nyasa, *Mem. II*, 172 pp., Geol. Surv. of Tanganyika, Dodoma, 1960.

Harkin, D. A., and J. R. Harpum, Quarter degree sheet 78 (Tukuyu), Geol. Surv. of Tanzania, Dodoma, 1978.

Heiken, G. H., Tuff rings: Examples from the Fort Rock–Christmas Lake valley region, south-central Oregon, *J. Geophys. Res., 76*, 5615–5626, 1971.

Johnson, T. C., T. W. Davies, B. M. Halfman, and N. D. Vaughan, Sediment core descriptions, Malawi '86, Project PROBE technical report, Duke Univ., Durham, N. C., 1988.

Kaufulu, Z., E. Vrba, and T. White, Age of the Chiwondo beds, northern Malawi, *Ann. Transvaal Mus., 33*, 1–8, 1981.

Kent, P. E., J. A. Hunt, and D. W. Johnstone, The geology and geophysics of coastal Tanzania, *Geophys. Pap. 6*, 101 pp., Inst. Geol. Sci. London, 1971.

King, B. C., Structural and volcanic evolution of the Gregory rift valley, in *Geologic Background to Fossil Man*, edited by W. W. Bishop, pp. 29–54, Scottish Academic, Edinburgh, 1978.

Klerkx, J., and J. T. Nanyaro, The Ukinga Group in southwestern Tanzania: A shear belt of Middle Proterozoic age?, *Inter. Geol. Correl. Prog. Newsl. 255* (1), 37–41, 1988.

Livingstone, D. A., Sedimentation and the history of water level change in Lake Tanganyika, *Limnol. Oceanogr., 10*, 607–610, 1965.

Macdonald, K. C., and P. J. Fox, Overlapping spreading centers: A new kind of accretionary plate boundary on the East Pacific Rise, *Nature, 302*, 55–58, 1983.

MacFarlane, A., Quarter degree sheet 258 and 258S (Itumba), Geol. Surv. Dep. of Tanganyika, Dodoma, 1963.

Morley, C. K., Variable extension in Lake Tanganyika, *Tectonics, 7*, 785–801, 1988.

Morley, C. K., Reply, *Tectonics, 8*, 651–653, 1989.

Pasteels, P., M. Villeneuve, P. DePaepe, and J. Klerkx, Timing of volcanism in the southern Kivu Province: Implications for the evolution of the western branch of the East African rift system, *Earth Planet. Sci. Lett.*, in press, 1989.

Peirce, J., and L. Lipkov, Structural interpretation of the Rukwa rift, Tanzania, *Geophysics, 53*, 824–836, 1988.

Pentel'kov, V., and S. Voronovskiy, Radiometric age of the Mbalizi carbonatite, Tanzania, and correlation with other carbonatites of the Rukwa-Malawi rift zone, *Dokl. Akad. Nauk SSSR, 235*, 1136–1139, 1977.

Pollard, D. D., and A. Aydin, Propagation and linkage of oceanic ridge segments, *J. Geophys. Res., 89*, 10,017–10,028, 1984.

Pouclet, A., Contribution a l'étude structurale de l'aïre volcanique des Virunga, rift de l'Afrique centrale, *Rev. Geogr. Phys. Geol. Dyn., XIX*, 115–124, 1977.

Quennell, A. M., A. C. M. McKinlay, and W. G. Aitken, Summary of the geology of Tanganyika, memoirs, 264pp., Mem. Geol. Surv. of Tanganyika., Dodoma, 1956.

Ray, G. E., The geology of the Chitipa-Karonga area, *Bull. Malawi Geol. Surv. Dep., 42*, 101 pp., 1975.

Reynolds, D., Structural and dimensional repetition in continental rifts, 166 pp., M.S. thesis, Duke Univ., Durham, N. C., 1984.

Rosendahl, B. R., D. J. Reynolds, P. Lorber, D. Scott, J. McGill, J. Lambiase, and S. J. Derksen, Structural expressions of rifting: Lessons from Lake Tanganyika, in *Sedimentation in the East African Rifts, Spec. Publ. 25*, edited by L. E. Frostick, pp. 29–34, Geological Society of London, 1986.

Rubin, A., and D. D. Pollard, Dike-induced faulting in rift zones of Iceland and Afar, *Geology, 16*, 413–417, 1988.

Shudofsky, G. N., Source mechanisms and focal depths of East African earthquakes using Rayleigh wave dispersion and body-wave modelling, *Geophys. J. R. Astron. Soc., 83*, 563–614, 1985.
Specht, T. D., Architecture of the Malaŵi rift, East Africa, 56 pp., M.S. thesis, Duke Univ., Durham, N. C., 1987.
Spence, J., The geology of the Galula coalfield, Mbeya district, *Tanganyika Geol. Surv. Dep. Bull. 25*, 33 pp., 1954.
Stockley, G. M., The geology of the north, west, and central Njombe district, Southern Highlands Province, *Tanganyika Geol. Surv. Dep. Bull., 18*, 67 pp., 1948.
Strecker, M. R., and P. M. Blisniuk, Rotation of extension direction in the central Kenya rift, paper presented at Symposium on the Afro-Arabian Rift System, [International Lithosphere Program], [Karlsruhe, F.R. Germany], 1989.
Taylor, J., *Introduction to Error Analysis*, p. 150, University Science Books, Mill Valley, California, 1982.
Teale, E. O., N. W. Eades, D. A. Harkin, J. R. Harpum, and R. G. Horne, Quarter degree sheet, 245 (Irambo), Geol. Surv. Dep. of Tanganyika, Dodoma, 1962.
Tiercelin, J. J., J. Chorowicz, H. Bellon, J.-P. Richert, J. T. Mwanbene, and F. Walgenwitz, East African rift system: Offset, age, and tectonic significance of the Tanganyika-Rukwa-Malaŵi intracontinental transcurrent fault zone, *Tectonophysics, 148*, 241–252, 1988.
Turcotte, D. L., and S. H. Emerman, Mechanisms of active and passive rifting, *Tectonophysics, 94*, 39–50, 1983.
Weissel, J. K., and G. D. Karner, Flexural uplift of rift flanks due to mechanical unloading of the lithosphere during extension, *J. Geophys. Res.*, in press, 1989.
WoldeGabriel, G., and J. L. Aronson, Chow Bahir rift: A "failed" rift in southern Ethiopia, *Geology, 15*, 430–433, 1987.
Wood, C. A., Morphometric evolution of cinder cones, *J. Volcanol. Geotherm. Res., 7*, 387–413, 1980.

A. L. Deino and R. E. Drake, Berkeley Geochronology Center, 2453 Ridge Road, Berkeley, CA 94709.
C. J. Ebinger, Geodynamics Branch, NASA Goddard Space Flight Center, Greenbelt, MD 20771.
A. L. Tesha, Department of Energy and Minerals, S. L. P. 903, Dodoma, Tanzania.

(Received October 12, 1988;
revised April 24, 1989;
accepted April 25, 1989)

[1]Now at Geodynamics Branch, NASA/Goddard Space Flight Center, Greenbelt, Maryland.

Paper number 89JB01088
0148-0227/89/89JB-01088$5.00

EBINGER ET AL.: RIFT PROPAGATION: RUNGWE, EAST AFRICA
EBINGER ET AL.: RIFT PROPAGATION: RUNGWE, EAST AFRICA
EBINGER ET AL.: RIFT PROPAGATION: RUNGWE, EAST AFRICA
EBINGER ET AL.: RIFT PROPAGATION: RUNGWE, EAST AFRICA
EBINGER ET AL.: RIFT PROPAGATION: RUNGWE, EAST AFRICA
EBINGER ET AL.: RIFT PROPAGATION: RUNGWE, EAST AFRICA
EBINGER ET AL.: RIFT PROPAGATION: RUNGWE, EAST AFRICA
EBINGER ET AL.: RIFT PROPAGATION: RUNGWE, EAST AFRICA
EBINGER ET AL.: RIFT PROPAGATION: RUNGWE, EAST AFRICA
EBINGER ET AL.: RIFT PROPAGATION: RUNGWE, EAST AFRICA
EBINGER ET AL.: RIFT PROPAGATION: RUNGWE, EAST AFRICA
EBINGER ET AL.: RIFT PROPAGATION: RUNGWE, EAST AFRICA
EBINGER ET AL.: RIFT PROPAGATION: RUNGWE, EAST AFRICA
EBINGER ET AL.: RIFT PROPAGATION: RUNGWE, EAST AFRICA
EBINGER ET AL.: RIFT PROPAGATION: RUNGWE, EAST AFRICA
EBINGER ET AL.: RIFT PROPAGATION: RUNGWE, EAST AFRICA
EBINGER ET AL.: RIFT PROPAGATION: RUNGWE, EAST AFRICA
EBINGER ET AL.: RIFT PROPAGATION: RUNGWE, EAST AFRICA
EBINGER ET AL.: RIFT PROPAGATION: RUNGWE, EAST AFRICA
EBINGER ET AL.: RIFT PROPAGATION: RUNGWE, EAST AFRICA
EBINGER ET AL.: RIFT PROPAGATION: RUNGWE, EAST AFRICA
EBINGER ET AL.: RIFT PROPAGATION: RUNGWE, EAST AFRICA
EBINGER ET AL.: RIFT PROPAGATION: RUNGWE, EAST AFRICA
EBINGER ET AL.: RIFT PROPAGATION: RUNGWE, EAST AFRICA

Fig. 1. Location of Rungwe volcanic province with respect to border faults and volcanic provinces of the Western and Kenya rifts and uplifted East African plateau [after *Ebinger*, 1989*a*]. Elevations above 800m enclosed by light line. Bold dashed line encloses Landsat-5 Thematic Mapper (TM) imagery from Rungwe volcanic province and field study region. Lake outlines serve as geographic references for subsequent figures. A–A' shows location of topographic profile shown in inset. Inset: Western and Kenya rifts have developed atop 1300-km-wide plateau. Shading emphasizes flanks of Western and Kenya rifts uplifted above 1300-m-high East African plateau.

Fig. 2. Geographic reference map of Rungwe region showing location of accommodation zones referred to in text, and Lakes Rukwa and Malawi (Nyasa) (Figure 1). R/S AZ is Rukwa-Songwe accommodation zone; S/K AZ is Songwe-Karonga accommodation zone; U/K AZ is Usangu-Karonga accommodation zone. Sediment cores T-2, and 86-30, 86-33 contain volcanic ashes described by *Livingstone* [1965] and *Johnson et al.* [1988], respectively. Border faults after *Ebinger et al.* [1987] and *Peirce and Lipkov* [1988].

Fig. 3. Geologic summary of Rungwe region showing general orientation of folds, shear zones, and metamorphic foliations (double light lines) within Precambrian and Archaean basement. Inset shows location of region within African continent. Triassic-Jurassic (Karroo) rift basins and Late Jurassic-Early Cretaceous sedimentary and volcanic sequences shaded. Geologic information from *Cahen and Snelling* [1984], *Daly et al.* [1989], *Harkin* [1955], *Kent et al.* [1971], *Klerkx and Nanyaro* [1988], and *Quennell et al.* [1956].

Fig. 4. Three-dimensional cartoon of the Rungwe volcanic province illustrating the morphology of accommodation zones between the Songwe, Usangu, and Karonga basins. Border fault (BF) scarps shown hatched; lacustrine sedimentary sequences and alluvium indicated by bold stipple pattern; Tertiary volcanics indicated by shading. Polyphase shield complexes and smaller centers indicated by cones and triangles, respectively. NW striking Mbaka transfer fault described in text. Vees point in direction of dip of monoclines. Bold arrows point in direction of basin asymmetry. Note: Southern tip of Lupa fault (Rukwa border fault) is located along uplifted flank of the Songwe basin.

Fig. 5. (Opposite) Geologic map of the Rungwe volcanic province and locations of volcanic rock samples dated in K-Ar analyses. Inset shows elevations (in meters above sea level) within Rungwe region. Structural information interpreted from enhanced Landsat TM imagery calibrated by field studies, aeromagnetic data, and gravity data; lithologic units as mapped and described by *Grantham et al.* [1958], *Harkin* [1960], *Teale et al.* [1962], *MacFarlane* [1963], *Ray* [1975], *Harkin and Harpum* [1978] (see also Figure 6). Faults beneath Lake Malawi interpreted from seismic reflection profiles [*Ebinger et al.*, 1984; *Specht*, 1987]. Bold arrows point to eastward offsets in rivers cited as evidence for ENE-striking fault system. Four corners of region shown in Figure 7 marked by dashed lines. Dashed line indicates location of cross section K–K' shown in Figure 9.

Fig. 6. Generalized stratigraphic sections within the Songwe, Usangu, and northern Karonga basin. Faunal ages of Lower Chiwondo beds (4–5 Ma) and Upper Chiwondo beds (2.4–2.6 Ma) from *Kaufulu et al.* [1981]; these units shown shaded. Tuff and ignimbrite flows indicated by quotation mark pattern; intrusive carbonatites indicated by c's. Vertical scale is units of time in millions of years (see Table 1); maximum reported thickness of sedimentary units indicated to left of column. Lithologic units modified after *Harkin* [1960], *Grantham et al.* [1958], and *Crossley* [1982].

Fig. 7. Portion of edge-enhanced Landsat TM image from the Mbaka fault zone along a segment of K–K' (Figure 9). Photo coverage shown in Figure 5. Note triangular scarps of metamorphic basement (B) along Mbaka fault that offset late Pleistocene basalt flows (Kb_2). Pliocene flows from shield volcanoes Tukuyu (To), Rungwe (Rt), and Kiejo (Kb) indicated. Arrows point to smaller (<100 m wide) pyroclastic cones and craters (e.g., Ob). Water-filled craters appear black in image; clouds are white.

Fig. 8. Gravity data from within the Rungwe region. (Top) Location of gravity stations. Open triangles: from *Aoki* [1969], *Fairhead and Sowerbutts* [1973], *Cowan and Pollack* [1977], and *Peirce and Lipkov* [1988]. Open circles: from compilation of C. Bowin, personal communication, 1987. (Bottom) Contours of Bouguer gravity calculated using crustal density of 2670 kg/m^3. Contour interval is 5 mGal; contours less than -160 mGal shaded. Bold dashed lines indicate location of Songwe (SBFS), Usangu (UBFS), and Karonga (KBFS) border fault segments. Arrow points to interpreted oblique-slip fault (C, Figure 10). Major shield volcanoes indicated by solid circles.

Fig. 9. Geologic cross section of the northern Karonga basin along line K–K' (Figure 5) illustrating geometry of southwestward tilted fault blocks and volcanic stratigraphy. Legend same as Figure 5. Mesozoic units (JR, K) shown shaded; estimate of depth to metamorphic basement based on extrapolation of bedding dips measured at surface. Note metamorphic basement exposed along Mbaka fault zone in central part of profile. Bold arrows point to locations of dated volcanic flow samples along or adjacent to profile K–K' (see Figure 5). Eruptive volcanic centers (e.g., maars, tuff rings, cinder cones) indicated by stars. Estimate of crustal extension along K–K' is 2–4 km. Inset: Sketch of crustal structure along K–K' based on depth to detachment estimate of ~20 km, location of volcanic centers, and assuming flexural uplift of the rift flanks.

Fig. 10. Spatial relationship between border and transfer faults and location of eruptive volcanic centers within the Rungwe province. *(a)* Border fault segments (BFS) indicated by bold lines; accommodation zones (structural highs) shown shaded; monoclines and relay ramps indicated by triangles pointing in direction of dip. Slip may be right or left lateral along parts of ENE striking oblique-slip faults interpreted at A, B, C. *(b)* Location of Late Miocene–Recent volcanic centers (solid circles) with respect to border faults (hatched lines) and transfer faults (light lines) (modified after *Harkin* [1960]). Ngozi, Rungwe, and Kiejo are major shield complexes; arrow north of Ngozi points along ENE strike of Poroto volcanic chain.

Fig. 11. Schematic diagram illustrating the location of eruptive volcanic centers throughout the late Miocene-Recent development of the Rukwa, Karonga, Songwe, and Usangu basins and accommodation zones. Bold lines indicate en echelon border fault segments; present-day outlines of Lakes Rukwa and Malawi (Nyasa) indicated by light lines. Sedimentary units indicated by bold stipple pattern; phonolitic/trachytic flows by light shading; alkali basalts by darker shading. *(a)* Volcanic activity begins at ~7 Ma at centers located near the present-day tips of the Karonga and Usangu border fault segments. Sediments begin to accumulate in the Rukwa and Karonga basins at 5–6 Ma. *(b)* Intrabasinal faulting and subsidence within the Usangu basin begins at ~2.5 Ma as volcanic centers become more numerous along the Mbaka transfer fault, and the ENE striking Poroto Mountain transfer fault links the Karonga and Usangu border fault segments. *(c)* Between 2.5 Ma and present, the Mbaka fault system propagated to the north. ENE striking transfer faults develop to link the newly formed Songwe border fault with the Karonga border fault segment to the south. With the development of the Songwe basin, the Rukwa and Karonga basins become linked, and the Usangu rift becomes a "failed" rift.

Fig. 12. Tectonic model of the Tanganyika-Rukwa-Malawi rift zone. Border fault segments indicated by bold lines; normal faults indicated by barbed lines; oblique-slip and strike-slip faults by light lines. Faults within the Rukwa region from *Peirce and Lipkov* [1988]; within Lake Tanganyika region, from *Ebinger* [1989*a*]. Shaded arrows indicate interpreted regional WSW-ENE extension direction. Focal mechanism solution of earthquake with epicentral location indicated by square shown as a lower hemisphere projection [from *Shudofsky*, 1985]. In late Miocene–Quaternary time the Malawi and Rukwa rifts became linked by the Songwe border fault segment and transfer faults within the Rukwa-Songwe and Songwe-Karonga accommodation zones. This propagation of en echelon border fault segments and a northward propagation of volcanism contribute to the along-axis segmentation of the Western rift valley.

Fig. 13. Temporal development of rift basins bounded by steep border fault systems. Stage 1: Phonolites/basalts (V1) erupt from fissures/incipient faults onto gentle topography. Subsidence occurs along border fault(s) and downwarping of basin commences. Stage 2: En echelon border faults displace originally flat-lying basalts and produce stair-step escarpment along one side of the basin. As intrabasinal fault systems develop, volcanic centers and flows (V2) localize to intrabasinal faults. Stage 3: Continued extension and fault block rotations occur within basins filling with sediments (S1, S2) and volcanics (V3). With progressive collapse of the hanging wall, slivers of the hanging wall are uplifted along with the flexurally uplifted flanks, and a new border fault system forms inside the older fault, effectively narrowing the basin (e.g., Figure 9, inset). This flank uplift tilts strata away from the rift valley. Because of their diachronous development, stage 1 roughly corresponds to the Songwe basin; stage 2, the Usangu basin; and stage 3, the Karonga basin.

Table 1. Potassium-Argon Ages: Rungwe Volcanic Province, Tanzania

Sample	Map; Rock Unit	K^+ Analyses	Weight (g)	K-A No.	$^{40}Ar^*$ (mol/g)	$\%^{40}Ar^*$	Age (Ma)	± (Ma)
T4D	Mb_p; Ol-basalt	0.652, 0.641	3.06684	5705-2	3.342E-12	35.2	2.98	0.09
				5705-3	3.419E-12	36.0	3.05	0.07
				5705-4	3.450E-12	36.4	3.07	0.07
				weighted mean			3.04	0.04
T5F	Mb_m; Ol-basalt	0.539, 0.553	1.71947	5706-2	6.597E-12	15.2	6.95	0.22
				5706-3	6.840E-12	15.8	7.21	0.27
				5706-4	6.882E-12	15.9	7.25	0.31
				weighted mean			7.10	0.15
T5K	Po; Ol-basalt	1.956, 1.945	6.19638	5709-2	1.913E-12	16.9	0.57	0.02
				5709-3	1.932E-12	17.1	0.57	0.02
				5709-4	1.922E-12	17.0	0.57	0.02
				weighted mean			0.57	0.01
T6C	St; trachyte[a]	5.382, 5.371	1.66154	5756-2	5.240E-12	19.2	0.56	0.02
				5756-3	5.088E-12	18.7	0.55	0.02
				weighted mean			0.55	0.01
T7A	Ot; trachyte[b]	4.724, 4.750	0.96982	5622	1.694E-11	48.9	2.20	0.2
T7H	Rg; trachyte	5.340, 5.349, 5.494	2.43839	5728-2	2.259E-12	16.4	0.24	0.01
				5728-3	2.363E-12	17.1	0.25	0.01
				5728-4	2.311E-12	16.8	0.25	0.01
				weighted mean			0.25	0.01
T8A	Rt; trachyte	4.926, 4.994	4.00487	5750-2	4.518E-13	2.1	0.050	0.013
				5750-3	5.581E-13	2.0	0.048	0.016
				5750-4	4.731E-13	2.1	0.050	0.014
				weighted mean			0.049	0.01
T8D	Ob_p; Ol-basalt	0.956, 0.876, 0.892	2.46401	5727-2	3.618E-12	11.0	2.30	0.13
				5727-3	3.507E-12	10.7	2.23	0.12
				5727-4	3.506E-12	10.7	2.23	0.12
				weighted mean			2.25	0.07
T9C	To; Ol-basalt[c]	0.723, 0.732	5.69569	5929-1	2.673E-12	35.5	2.12	0.06
				5929-2	2.672E-12	35.5	2.12	0.05
				weighted mean			2.12	0.04
T10G	Kb_1; picrite	1.115, 1.171	5.28529	5749-2	7.943E-13	1.8	0.40	0.10
				5749-3	8.387E-13	1.9	0.42	0.03
				5749-4	8.792E-13	2.0	0.44	0.08
				weighted mean			0.42	0.03
T10H	Kg; trachyte	0.993, 0.899, 0.967	2.47375	5707-2	5.726E-13	4.2	0.35	0.05
				5707-3	5.877E-13	4.3	0.36	0.06
				5707-4	6.894E-13	5.1	0.42	0.09
				weighted mean			0.36	0.03
T11A	Kat; trachyte[b]	5.206, 5.191	0.75726	5703	2.121E-11	49.3	2.35	0.04
T13F	Et; trachyte[b]	4.732, 4.724	1.15372	5621	1.934E-11	24.7	7.25	0.6
T14A	To; Ol-basalt	0.941, 0.958	2.76676	5744-2	2.687E-12	17.6	1.63	0.13
				5744-3	2.690E-12	17.5	1.63	0.09
				5744-4	2.700E-12	17.6	1.64	0.12
				weighted mean			1.63	0.06
T14B	Kb_2; Ol-basalt	0.859, 0.862	4.03080	5725-2	1.062E-13	0.2	0.07	0.22
				5725-3	1.713E-13	0.4	0.12	0.13
				weighted mean			0.10	0.11
T15A	Ob_p; ankaramite	1.110, 1.086	4.02237	5724-3	4.410E-12	22.7	2.32	0.08
				5724-6	4.344E-12	22.3	2.28	0.06
				weighted mean			2.29	0.05
T15B	Ob_m; Ol-basalt	0.930, 0.960	2.71566	5746-2	9.085E-12	6.9	5.54	0.36
				5746-3	8.622E-12	6.5	5.25	0.35
				5746-4	9.149E-12	6.9	5.58	0.38
				weighted mean			5.45	0.21

Decay constants: $\lambda_\varepsilon + \lambda_{\varepsilon'} = 0.581 \times 10^{-10}\ yr^{-1}$; $\lambda_\beta = 4.962 \times 10^{-10}\ yr^{-1}$; $\lambda = 5.543 \times 10^{-10}\ yr^{-1}$; $^{40}K/K = 0.01167\%$. $^{40}Ar^*$ (columns 6 and 7) refers to radiogenic component.

[a] Anorthoclase separate.

[b] Dated prior to reconfiguration of extraction line/spectrometer.

[c] Analyses 5929-1, 5929-2 done at a later date; gas fractions in both analyses were equal in volume (see text).

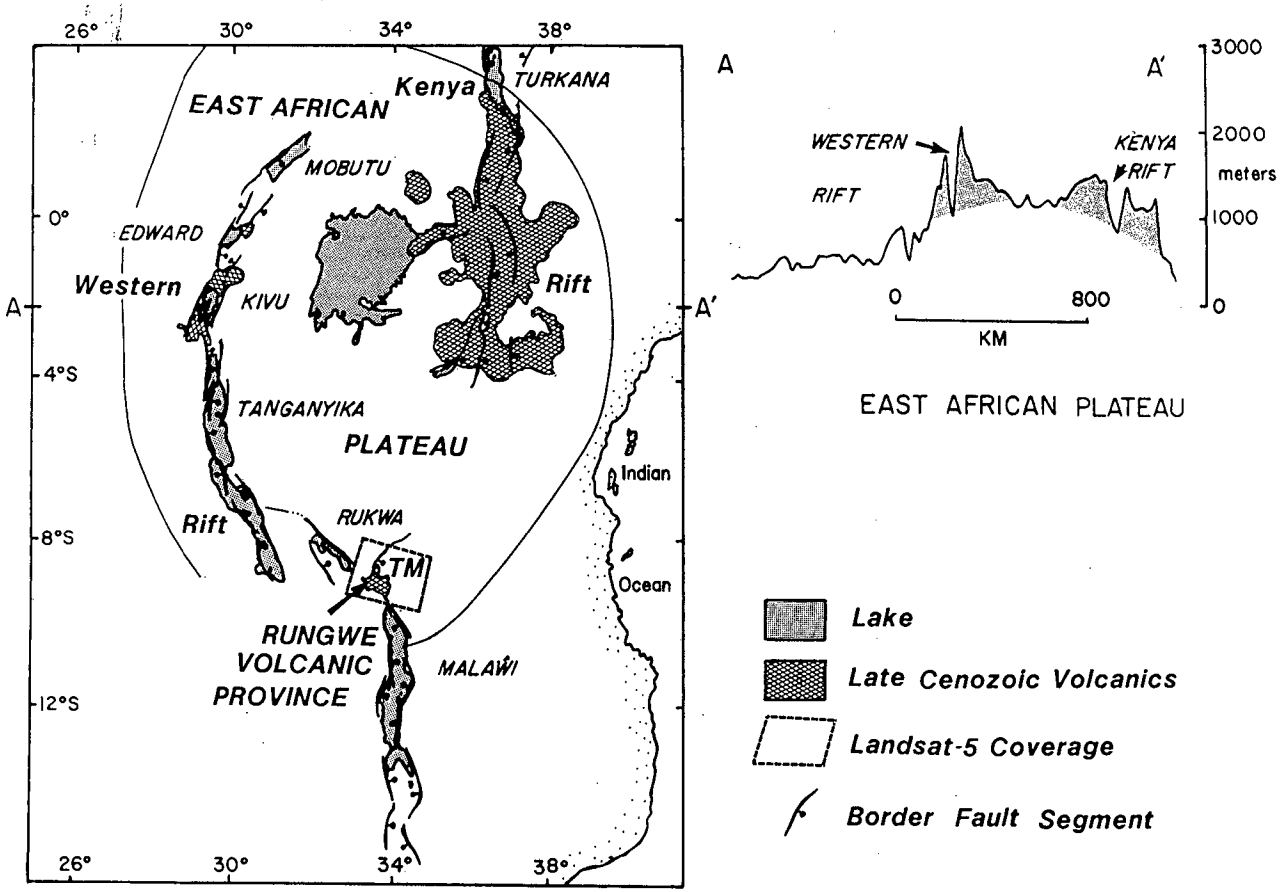
26°
30°
34°
38°
EAST AFRICAN
Kenya
TURKANA
MOBUTU
0°
EDWARD
Western
KIVU
Rift
A
A'
4°S
TANGANYIKA
PLATEAU
Indian
Rift
RUKWA
8°S
TM
Ocean
RUNGWE
VOLCANIC
PROVINCE
MALAWI
12°S
26°
30°
34°
38°
A
A'
3000
2000
meters
1000
0
WESTERN
RIFT
KENYA
RIFT
0
800
KM
EAST AFRICAN PLATEAU
Lake
Late Cenozoic Volcanics
Landsat-5 Coverage
Border Fault Segment

Fig. 1

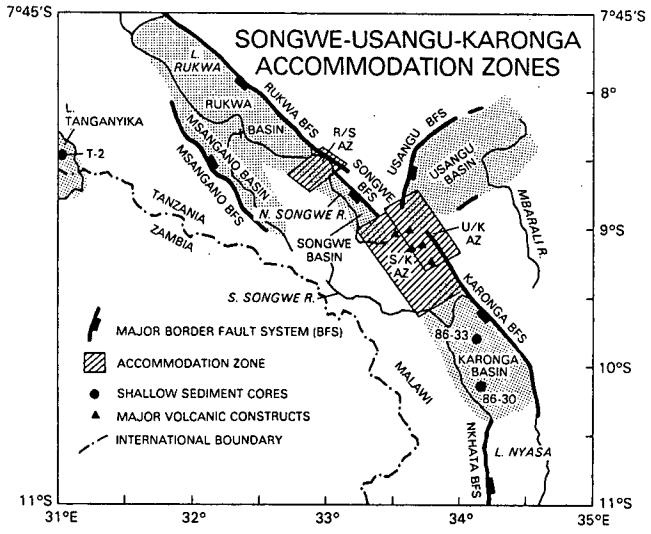
SONGWE-USANGU-KARONGA
ACCOMMODATION ZONES
7°45'S
7°45'S
8°
9°S
10°S
11°S
11°S
31°E
32°
33°
34°
35°E
L. RUKWA
RUKWA BFS
RUKWA BASIN
R/S AZ
L. TANGANYIKA
T-2
MSANGANO BASIN
MSANGANO BFS
N. SONGWE R.
SONGWE BFS
USANGU BFS
USANGU BASIN
MBARALI R.
TANZANIA
ZAMBIA
SONGWE BASIN
U/K AZ
S/K AZ
KARONGA BFS
S. SONGWE R.
86-33
KARONGA BASIN
86-30
MALAWI
NKHATA BFS
L. NYASA
MAJOR BORDER FAULT SYSTEM (BFS)
ACCOMMODATION ZONE
SHALLOW SEDIMENT CORES
MAJOR VOLCANIC CONSTRUCTS
INTERNATIONAL BOUNDARY

Fig. 2

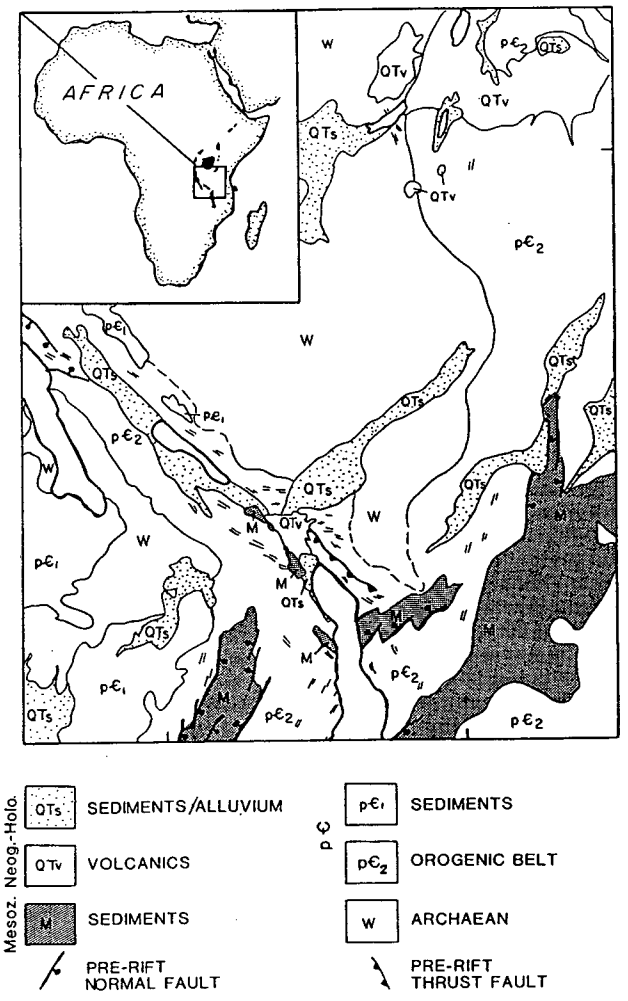

FIG. 3
EBINGER

SONGWE · USANGU · KARONGA ACCOMMODATION ZONE

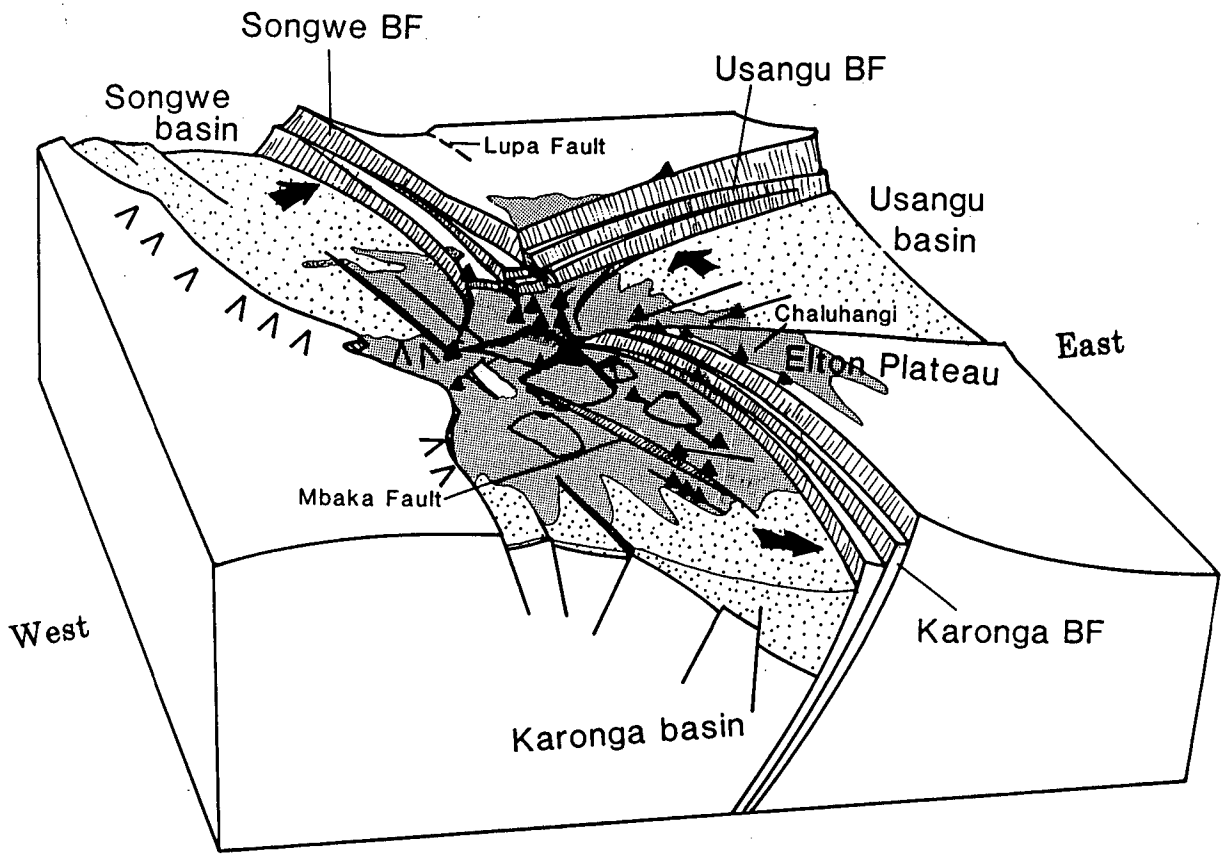

FIG. 4
EBINGER

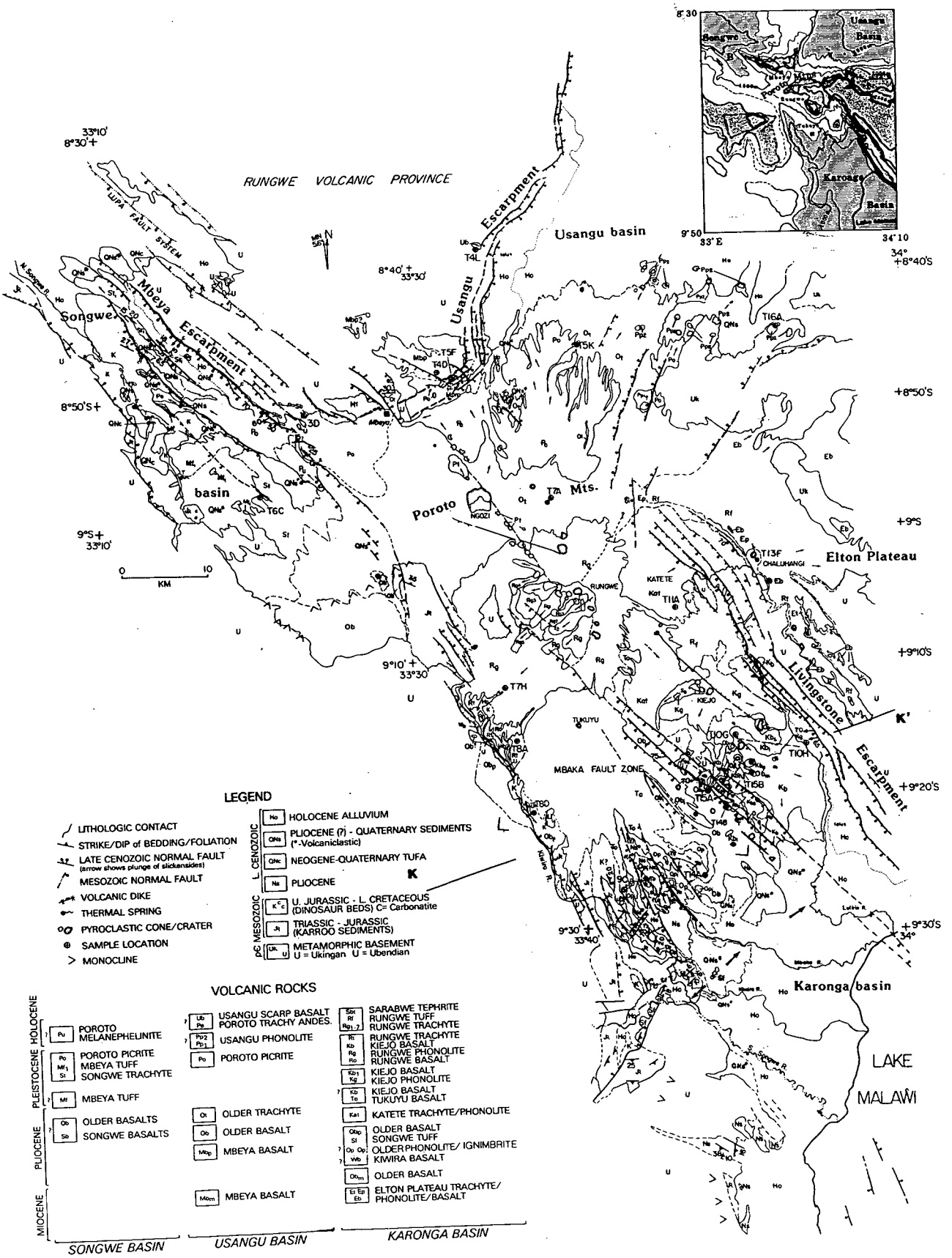

FIG. 5
EBINGER

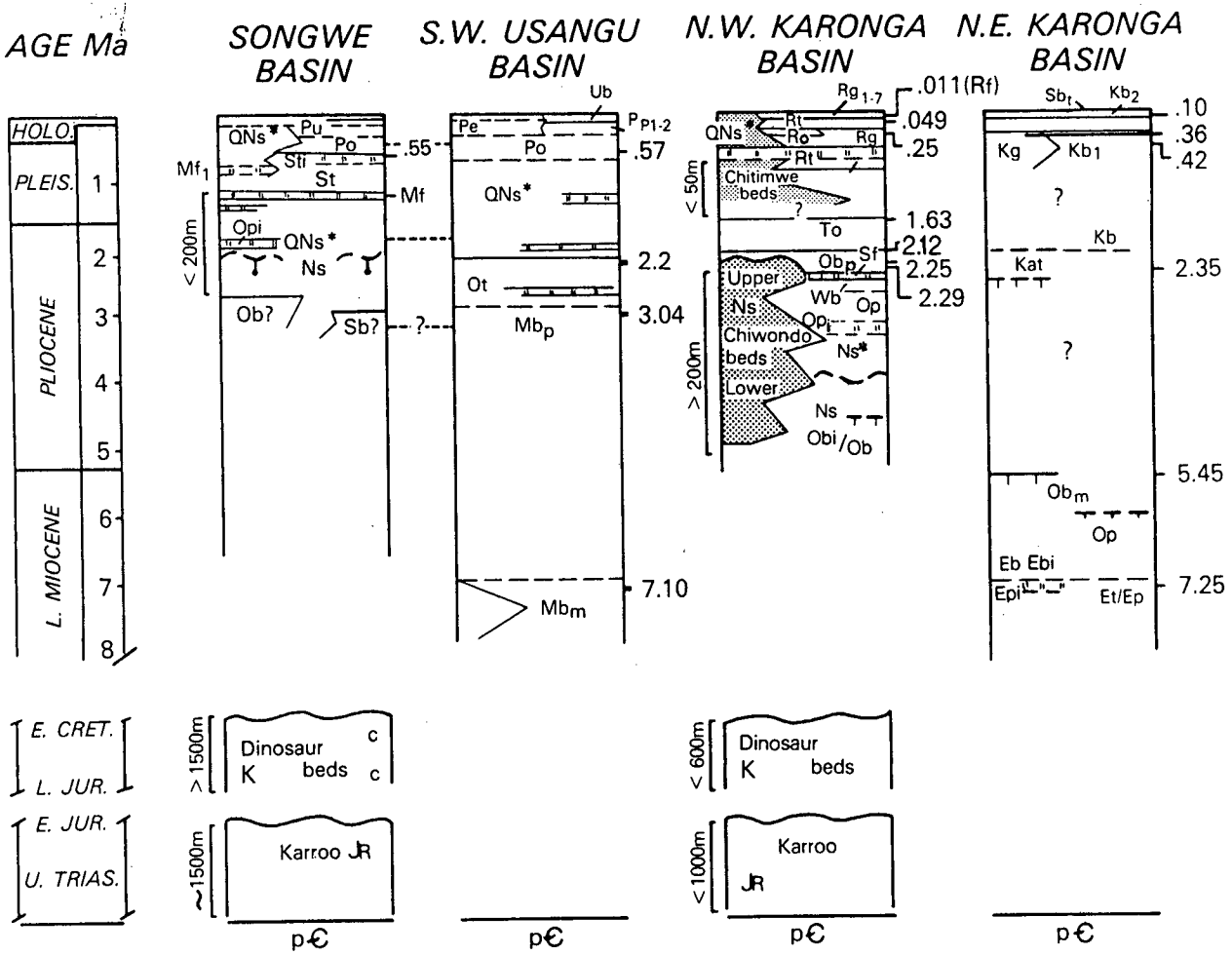

FIG. 6
EBINGER

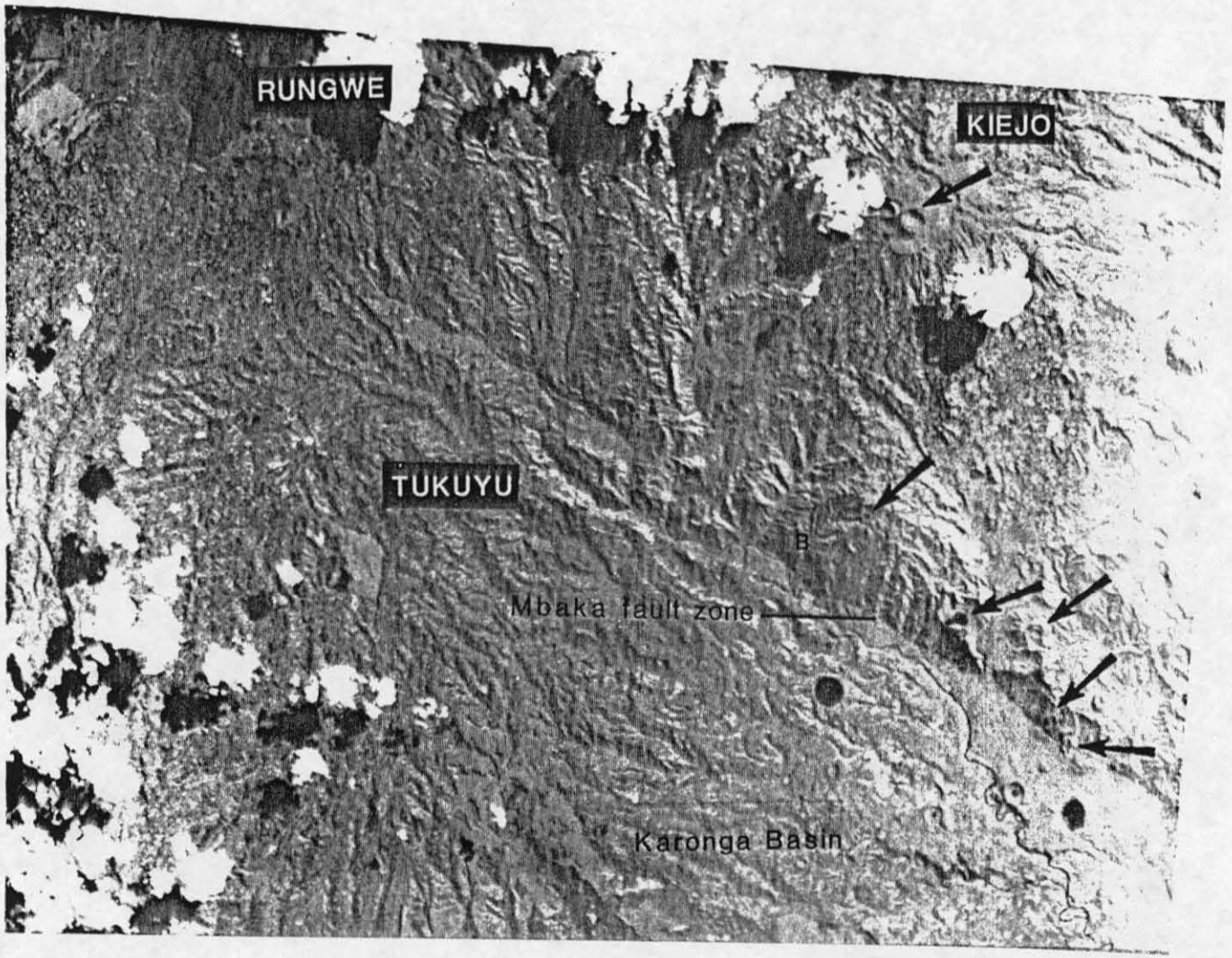
RUNGWE
KIEJO
TUKUYU
B
Mbaka fault zone
Karonga Basin

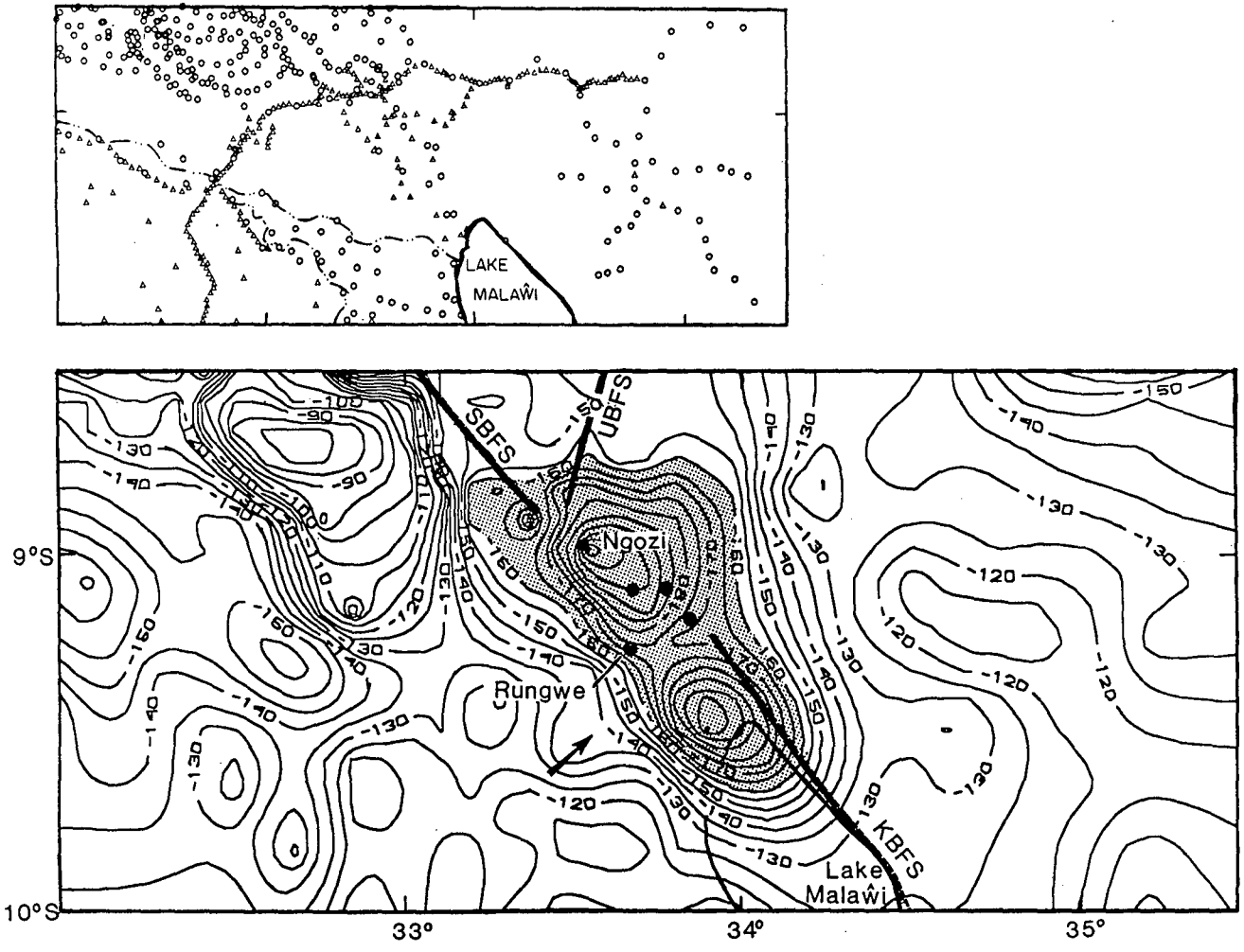

FIG. 8
EBINGER

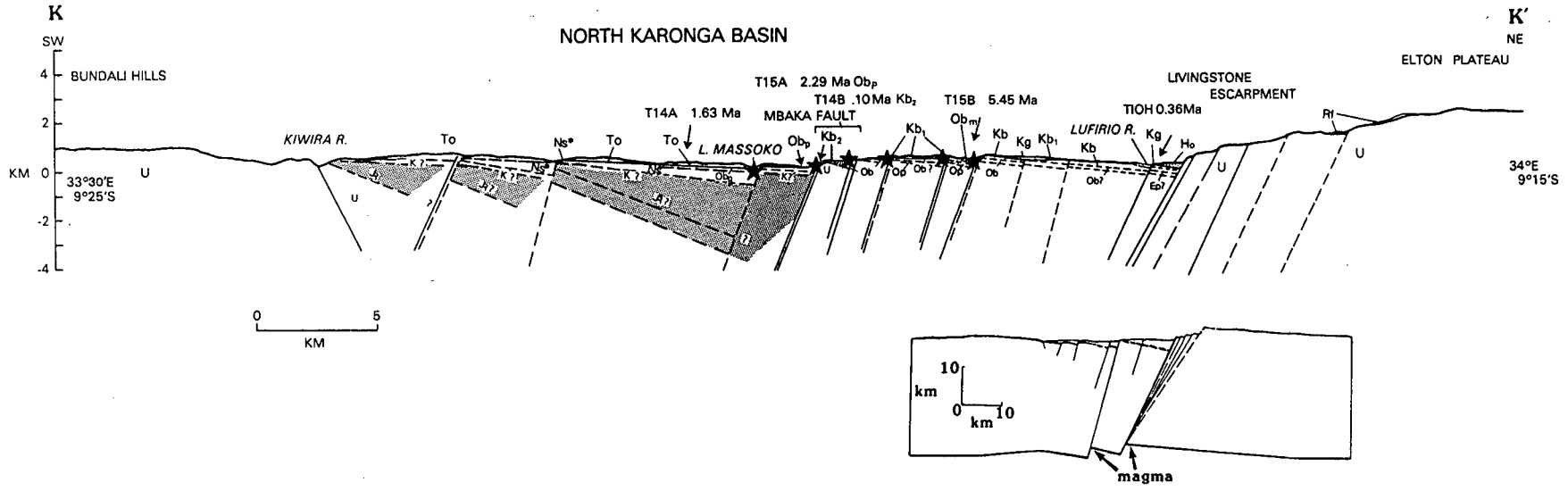

FIG 9
EBINGER

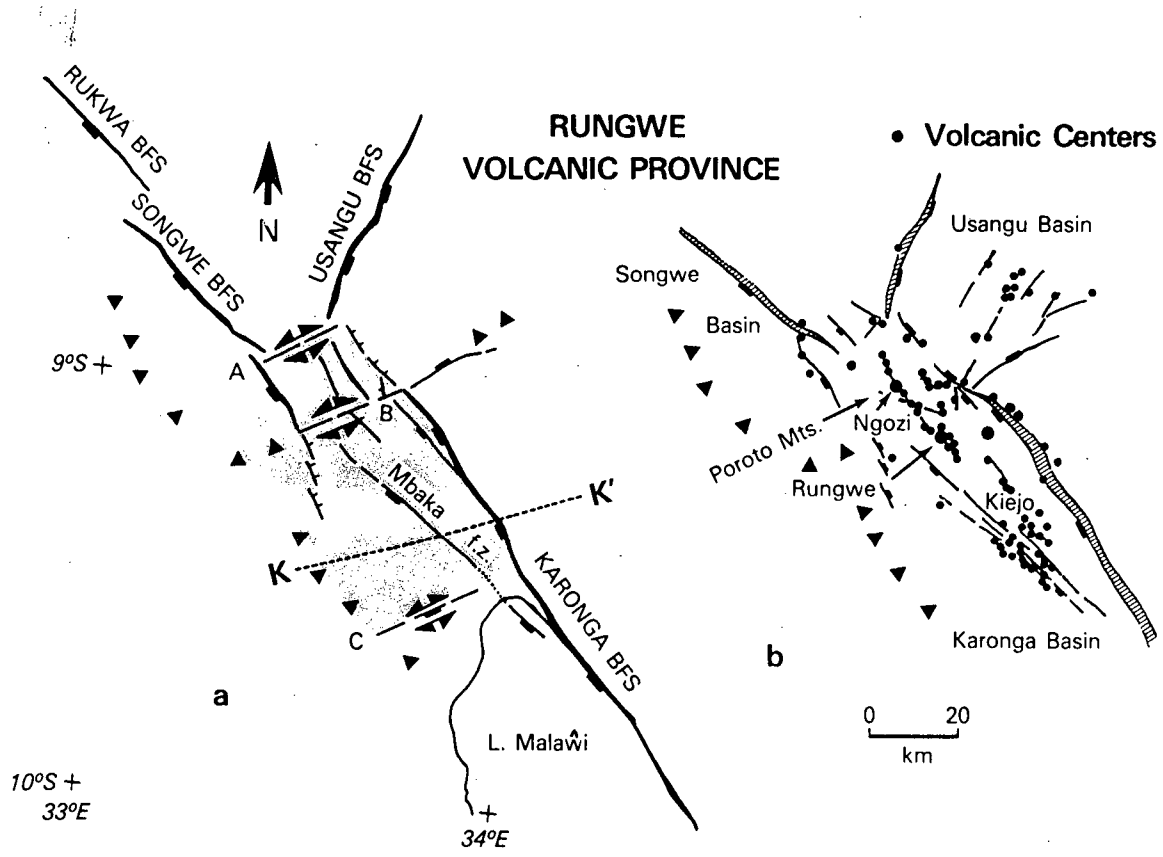

FIG.10
EBINGER

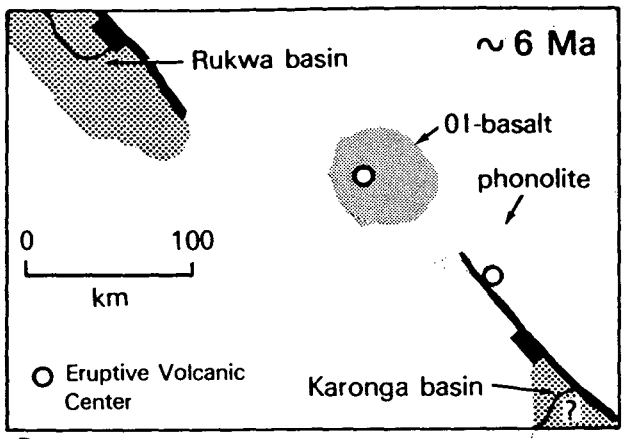

A

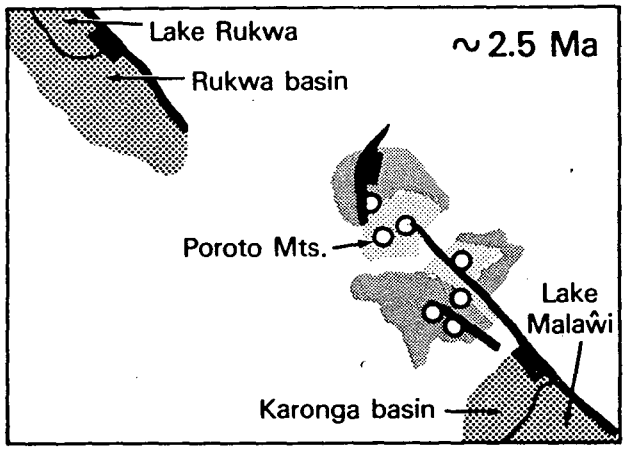

B

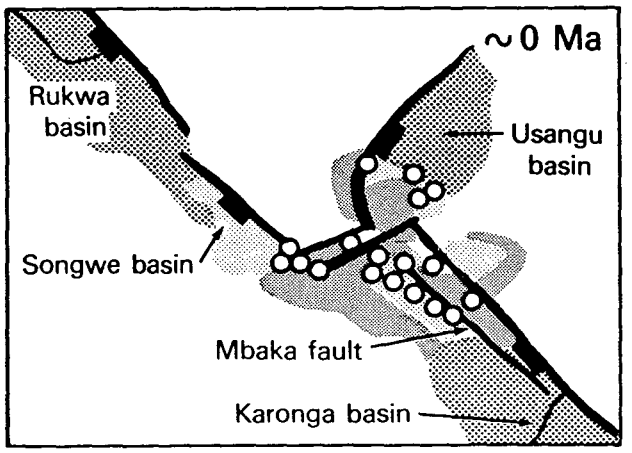

C

FIG. 11
EBINGER

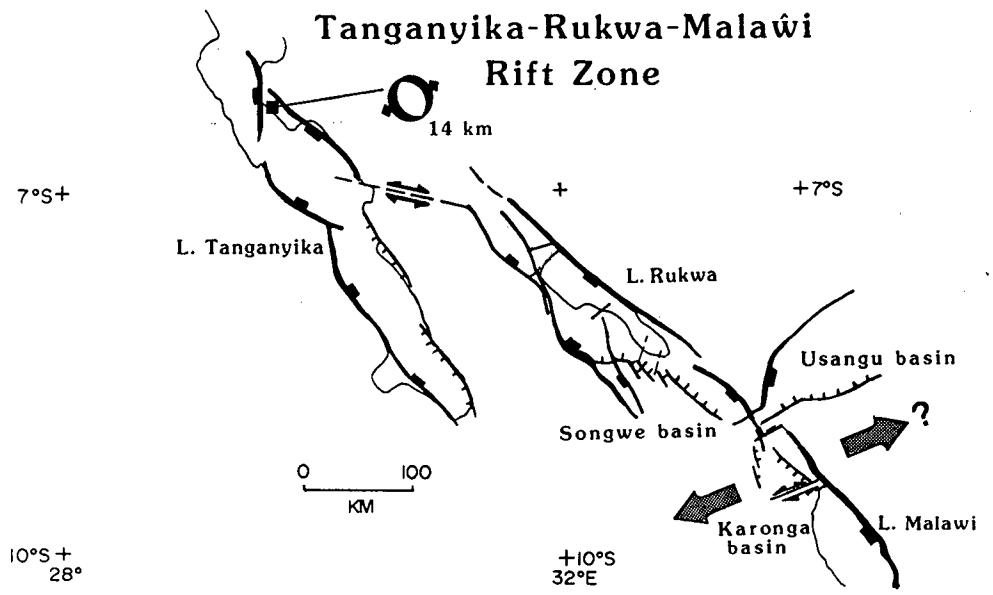

FIG. 12
EBINGER

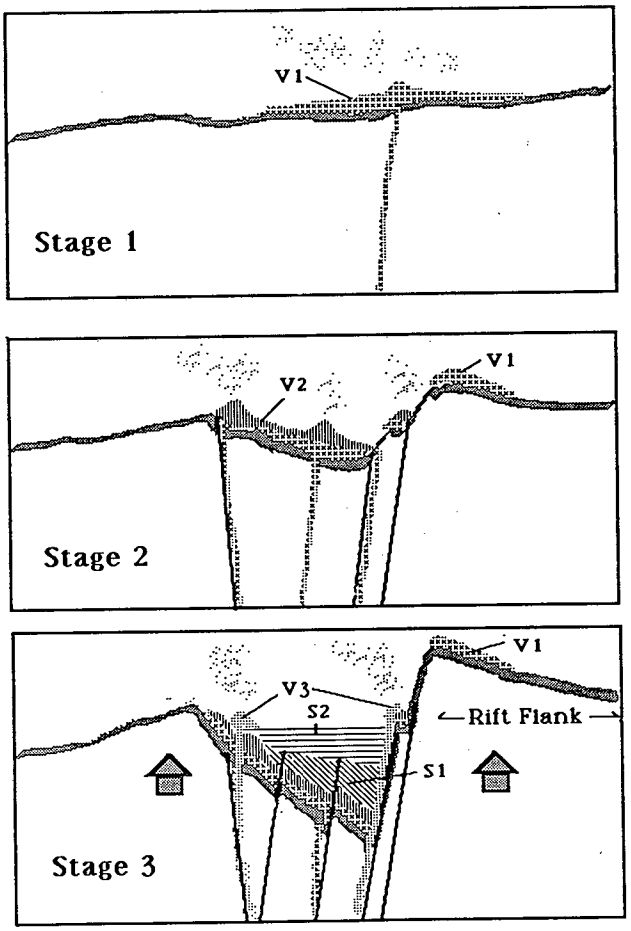

FIG. 13
EBINGER